

Higgs boson property measurements with $H \rightarrow \gamma\gamma$ at CMS



Junquan Tao (IHEP/CAS)
on behalf of the *CMS collaboration*
in particular the *joint IP2I+IHEP team*



中国科学院高能物理研究所
Institute of High Energy Physics
Chinese Academy of Sciences

16th France-China Particle Physics Network/Laboratory workshop (FCPPN/L 2025)

21–25 July, 2025

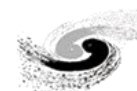
Haitian Grand Theatre Hotel, Qingdao



中国科学院
CHINESE ACADEMY OF SCIENCES



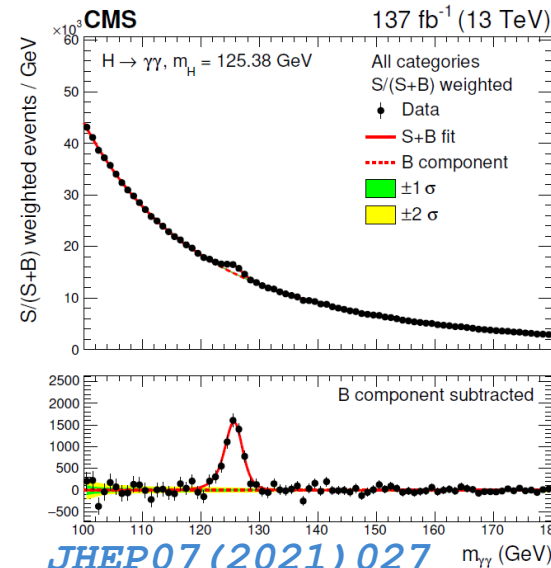
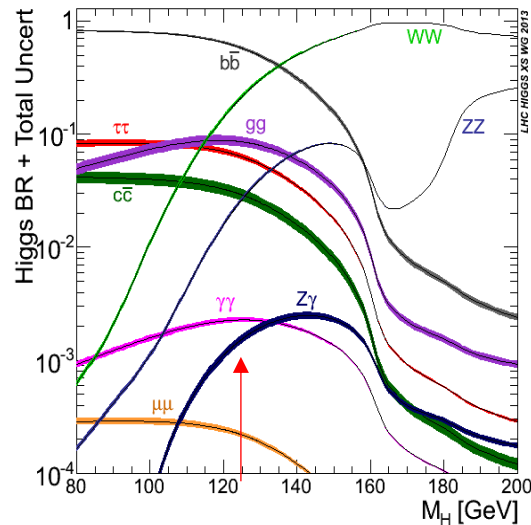
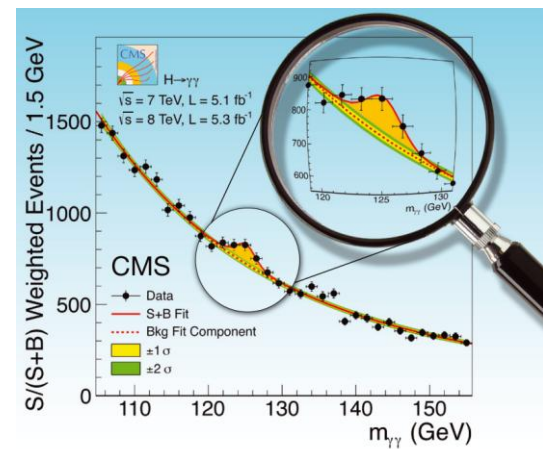
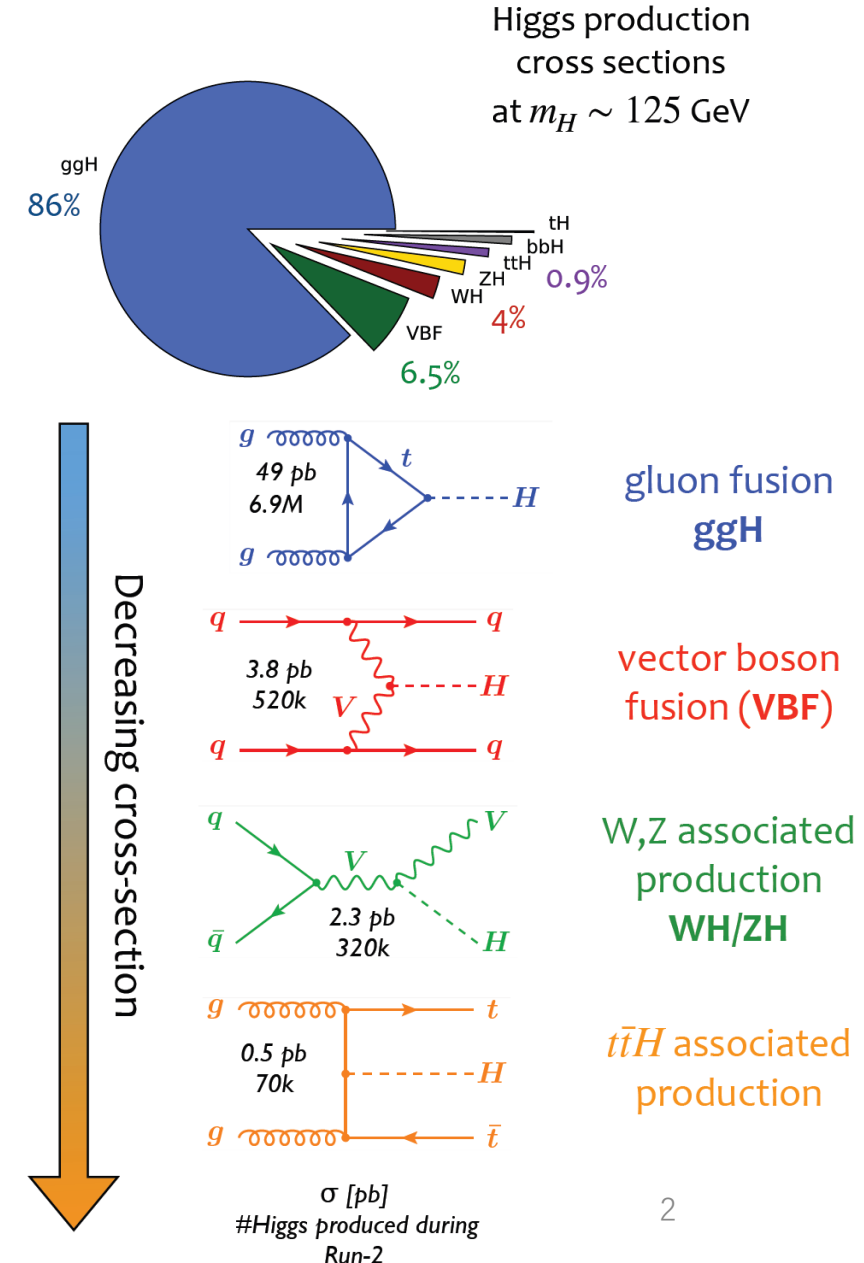
中国高等科学技术中心
China Center of Advanced Science and Technology



中国科学院高能物理研究所
Institute of High Energy Physics Chinese Academy of Sciences

Introduction

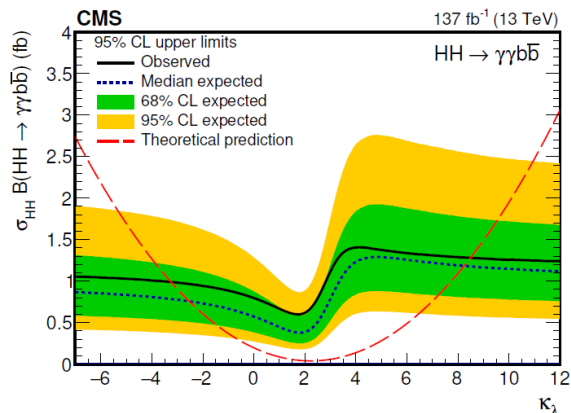
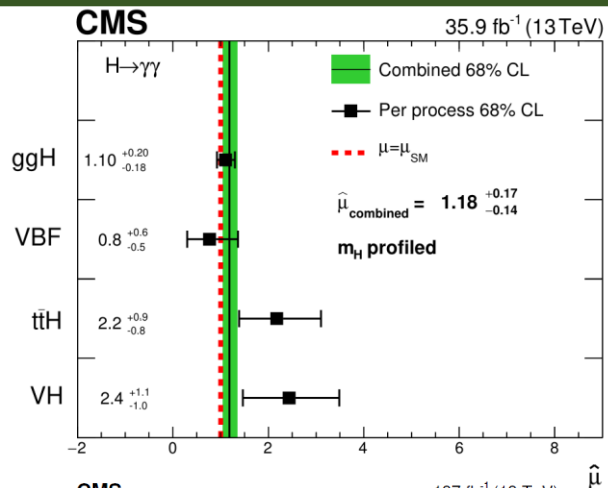
- **LHC is a Higgs factory**
- About **8 million Higgs bosons** produced by LHC during Run2 ($\sqrt{s} = 13$ TeV) **per experiment**
- **$H \rightarrow \gamma\gamma$** is one of the **golden channels** in the **Higgs boson discovery** and its **property measurements**, and also search for additional resonances (Benjamin's [talk](#))
 - ✓ **Small branching ratio** $\sim 0.23\%$
 - ✓ **Clean final state** fully reconstructed with high energy resolution and $m_{\gamma\gamma}$ resolution (1-2%)





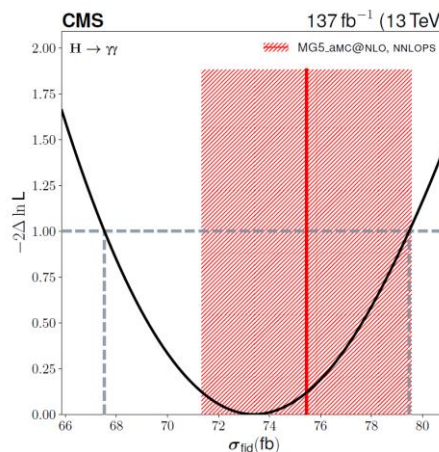
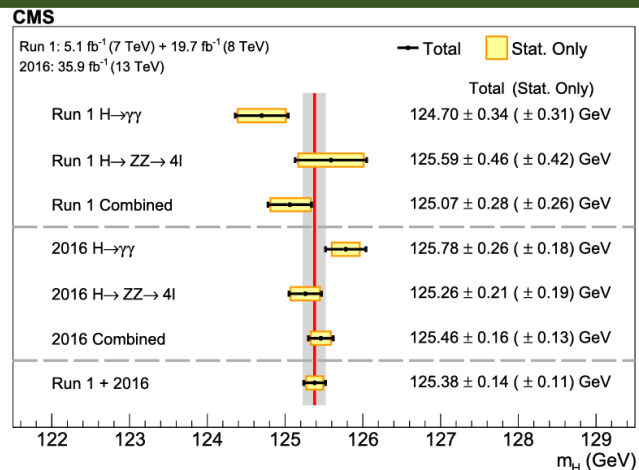
Roadmap of Run2 $H \rightarrow \gamma\gamma$ measurements

HIG-16-040 ([JHEP11\(2018\)185](#)):
signal strength with 2016 data



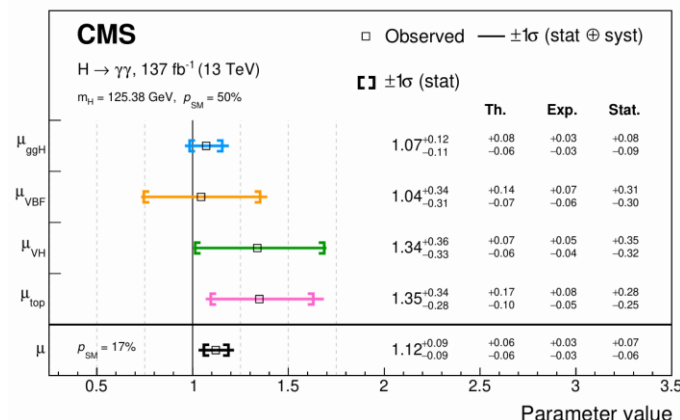
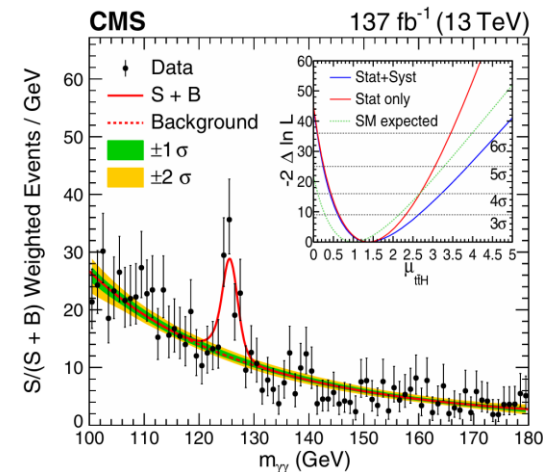
Self coupling in non-resonant HH
HIG-19-018 ([JHEP03\(2021\)257](#)): $HH \rightarrow b\bar{b}\gamma\gamma$
HIG-21-014: $HH \rightarrow WW\gamma\gamma$
HIG-22-012 ([arXiv:2506.23012](#)): $HH \rightarrow \gamma\gamma\tau\tau$

HIG-19-004 ([PLB805\(2020\)135425](#)):
mass with 2016 data



HIG-19-016 ([JHEP07\(2023\)091](#)):
fiducial cross section (XS) and
differential fiducial XS

HIG-19-013 ([PRL 125 \(2020\) 061801](#)):
Full Run2 **ttH(→γγ)** **observation + CP**



HIG-19-015 ([JHEP07\(2021\)027](#)):
**signal strengths & Simplified
Template Cross Section (1.2)**

Analyses covered in this talk

Including the latest $H \rightarrow \gamma\gamma$ results released in last ~1 year

- [HIG-23-014](#) ([arxiv:2504.17755](#)): $H \rightarrow \gamma\gamma$ **fiducial and differential cross section** with **Run3 data**
 - ✓ First Run3 $H \rightarrow \gamma\gamma$ analysis/paper, released for ICHEP2024
- [HIG-23-010](#) ([arXiv:2503.08797](#)): $H(\rightarrow \gamma\gamma) + c$ to probe **Higgs-charm coupling** with **Run2 data**
 - ✓ First search for cH , $H \rightarrow \gamma\gamma$ at LHC, released for ICHEP2024
- [HIG-24-006](#) : **Anomalous couplings** in VH, VBF, ggH with $H \rightarrow \gamma\gamma$ and **Run2 data**

Many ongoing analyses with $H \rightarrow \gamma\gamma$:

- ✓ Run2 mass and width (HIG-24-007, HIG-25-004)
- ✓ Run2 HHH- \rightarrow 4b2 γ (HIG-24-015) to constrain self-coupling λ_3 and λ_4
- ✓ Run3 HH- \rightarrow bb $\gamma\gamma$ to probe self-coupling λ_3
- ✓ ...

Run-2
~140 fb⁻¹
(2016-2018, $\sqrt{s} = 13$ TeV)

“early” Run-3
(2022-2023)

~60 fb⁻¹

(2022-2026, $\sqrt{s} = 13.6$ TeV)

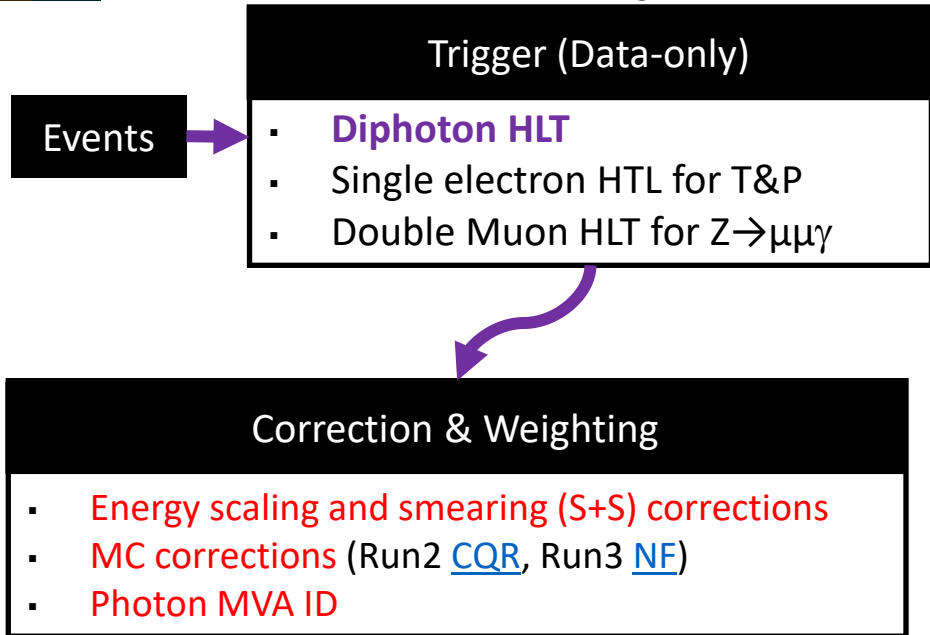
Run-3 2024

~100 fb⁻¹

4

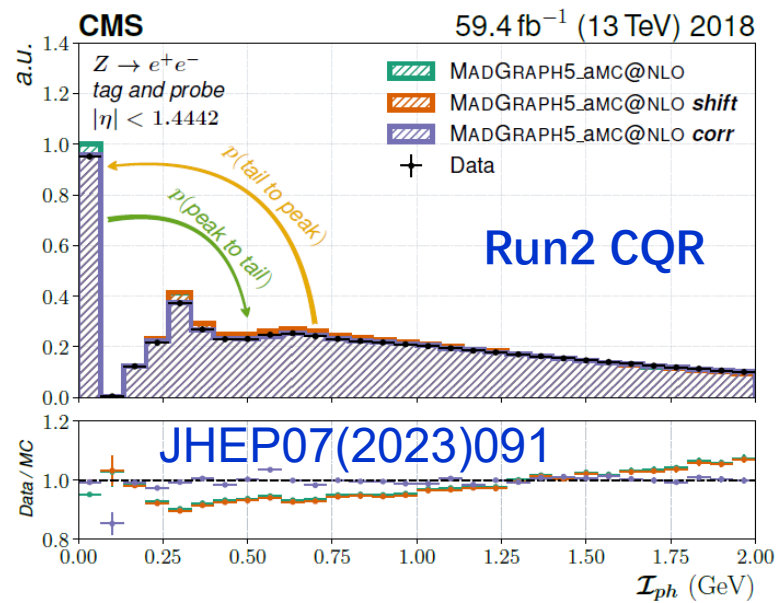
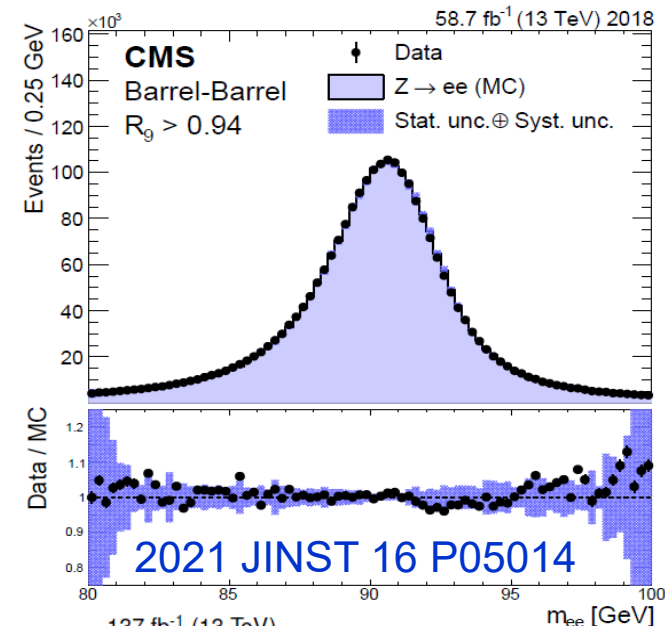
Very new:
released for
EPS2025 (July)

Analysis Workflow and Strategy



Energy scaling and smearing: using $Z \rightarrow ee$ events with electrons reconstructed as photons

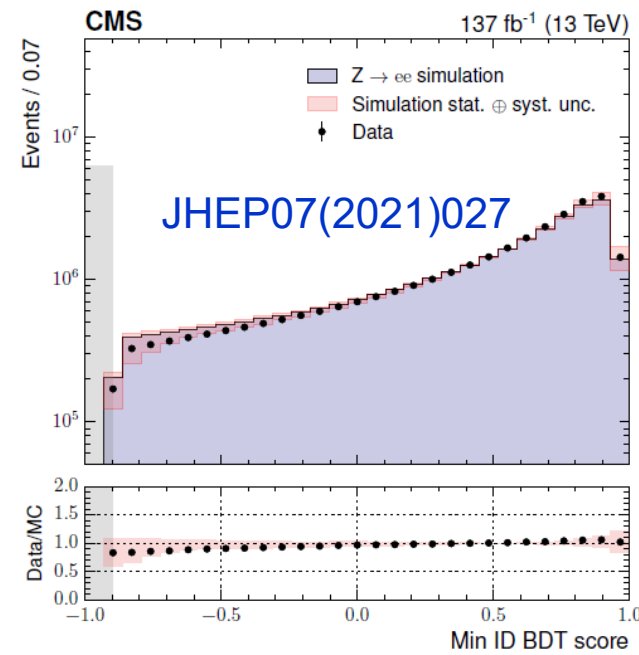
Per object strategy



MC corrections to improve data/MC agreements

Run2: *Chained Quantile Regression* ([arXiv:1211.6581](#), extremely complicated and time-consuming)

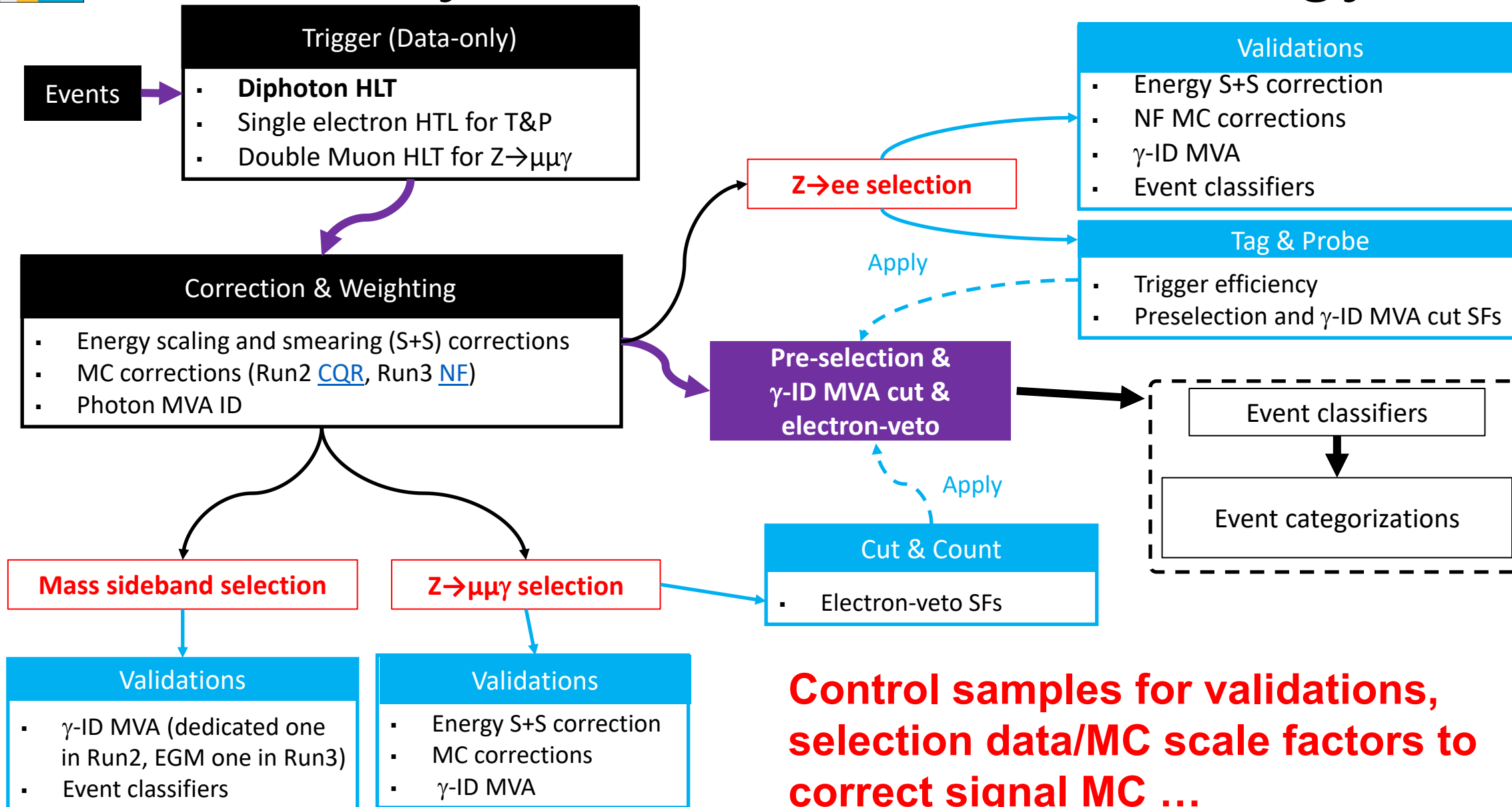
Run3: *Normalizing flow* ([arXiv:2403.18582](#))



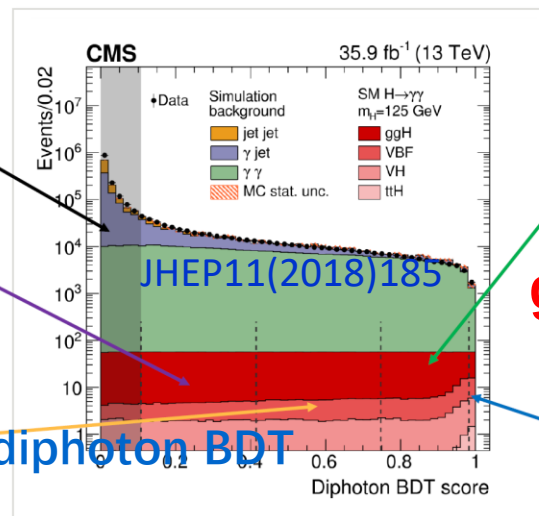
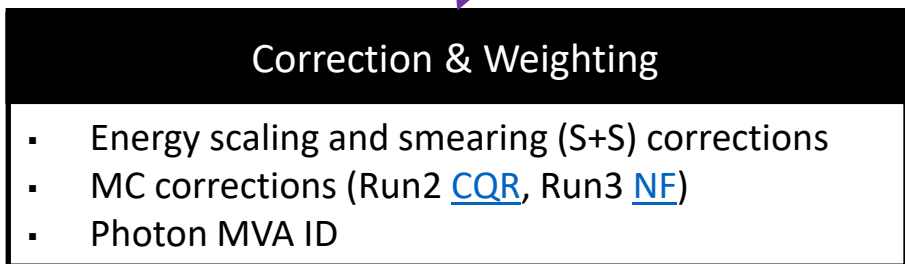
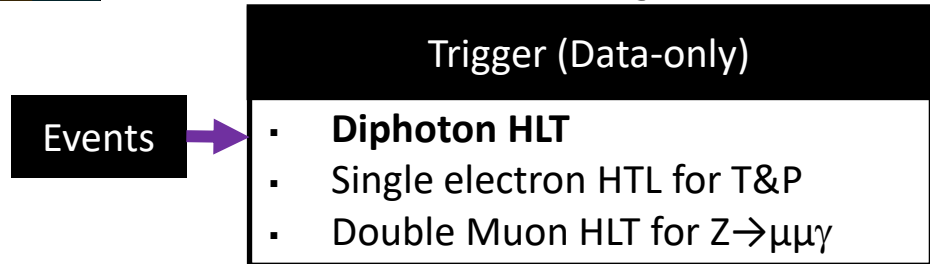
Photon ID MVA trained to distinguish prompt photons from jets

Validated on $Z \rightarrow ee$ and $Z \rightarrow \mu\mu\gamma$ data/MC

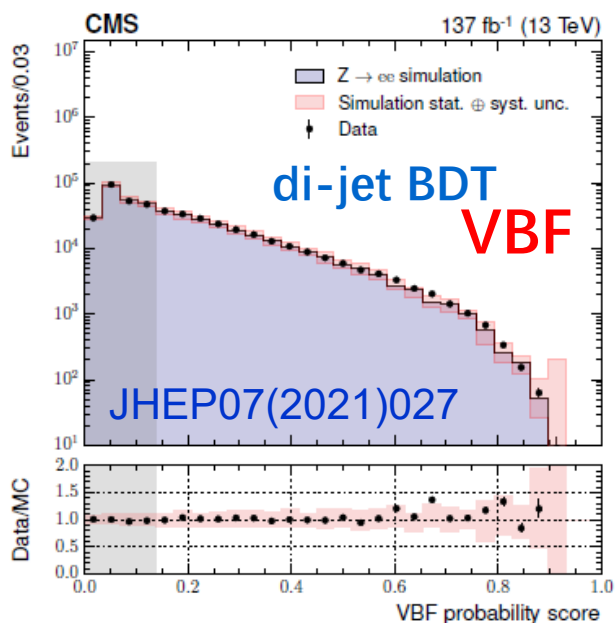
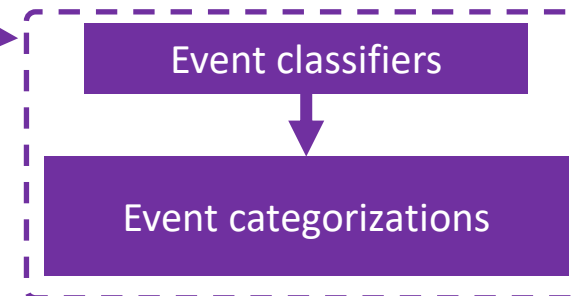
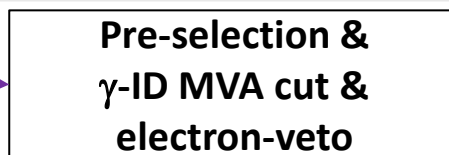
Analysis Workflow and Strategy



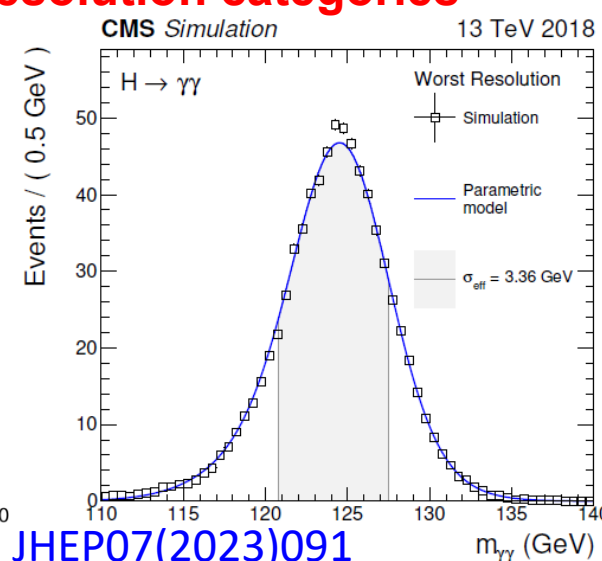
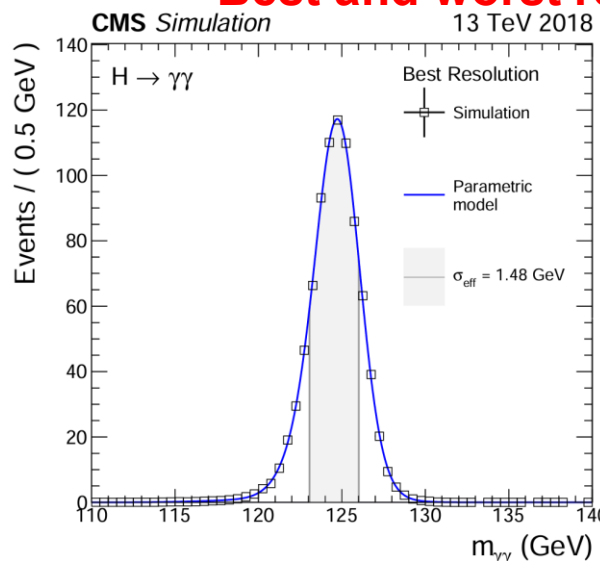
Analysis Workflow and Strategy



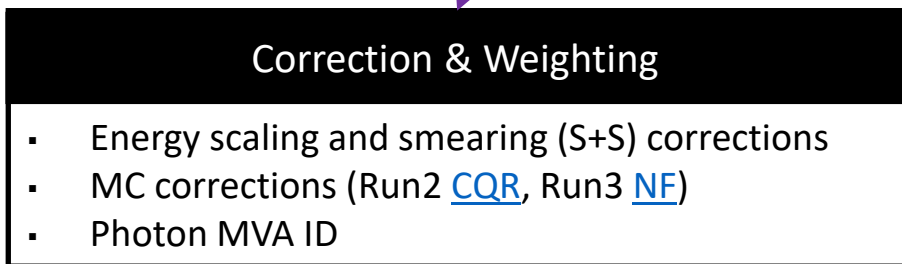
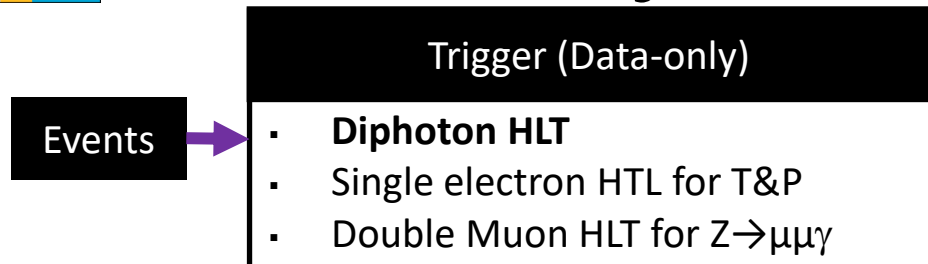
Event categorization
on production modes,
mass resolution and
S/B to improve the
analysis sensitivity



Best and worst resolution categories

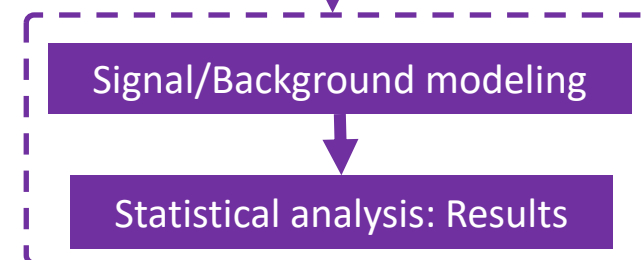
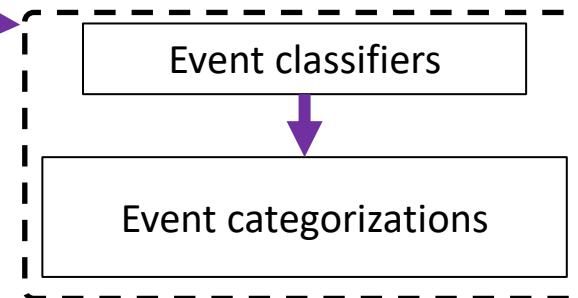
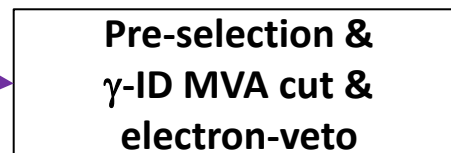
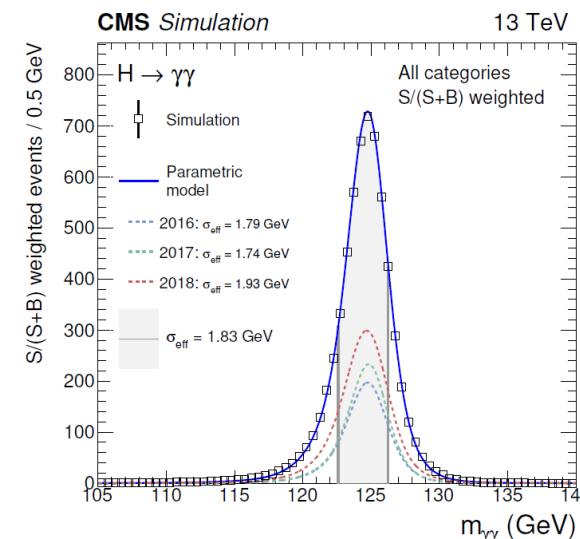


Analysis Workflow and Strategy

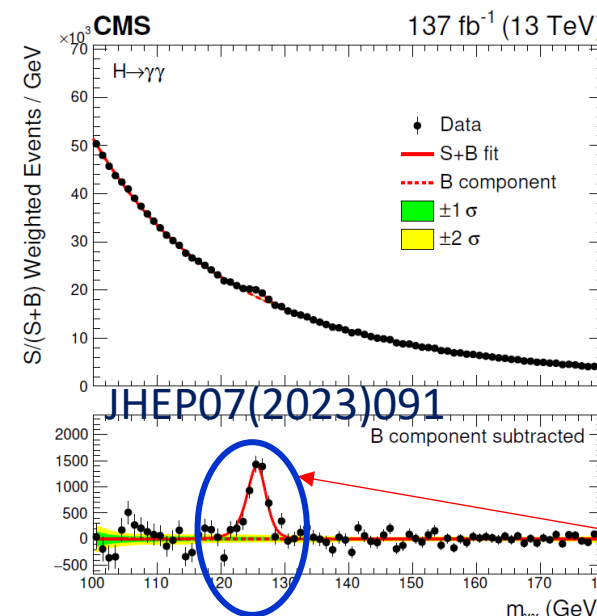
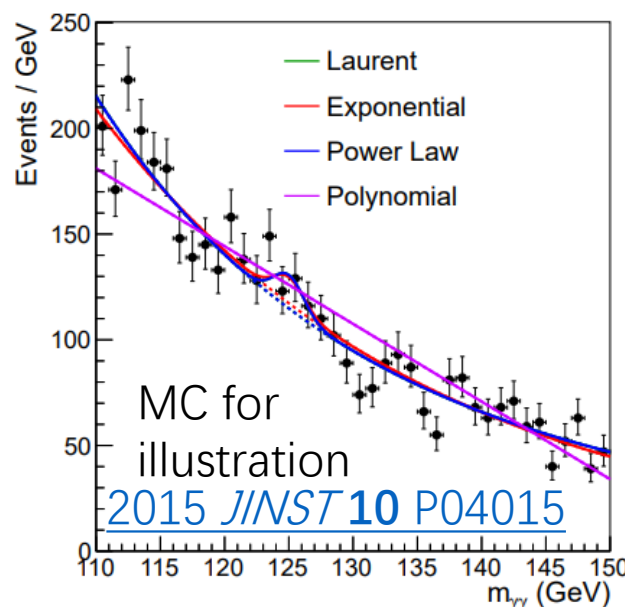


Sig and bkg modeling based on $m_{\gamma\gamma}$

Signal model derived from MC simulation, with corrections (trigger eff, data/SFs, ...)

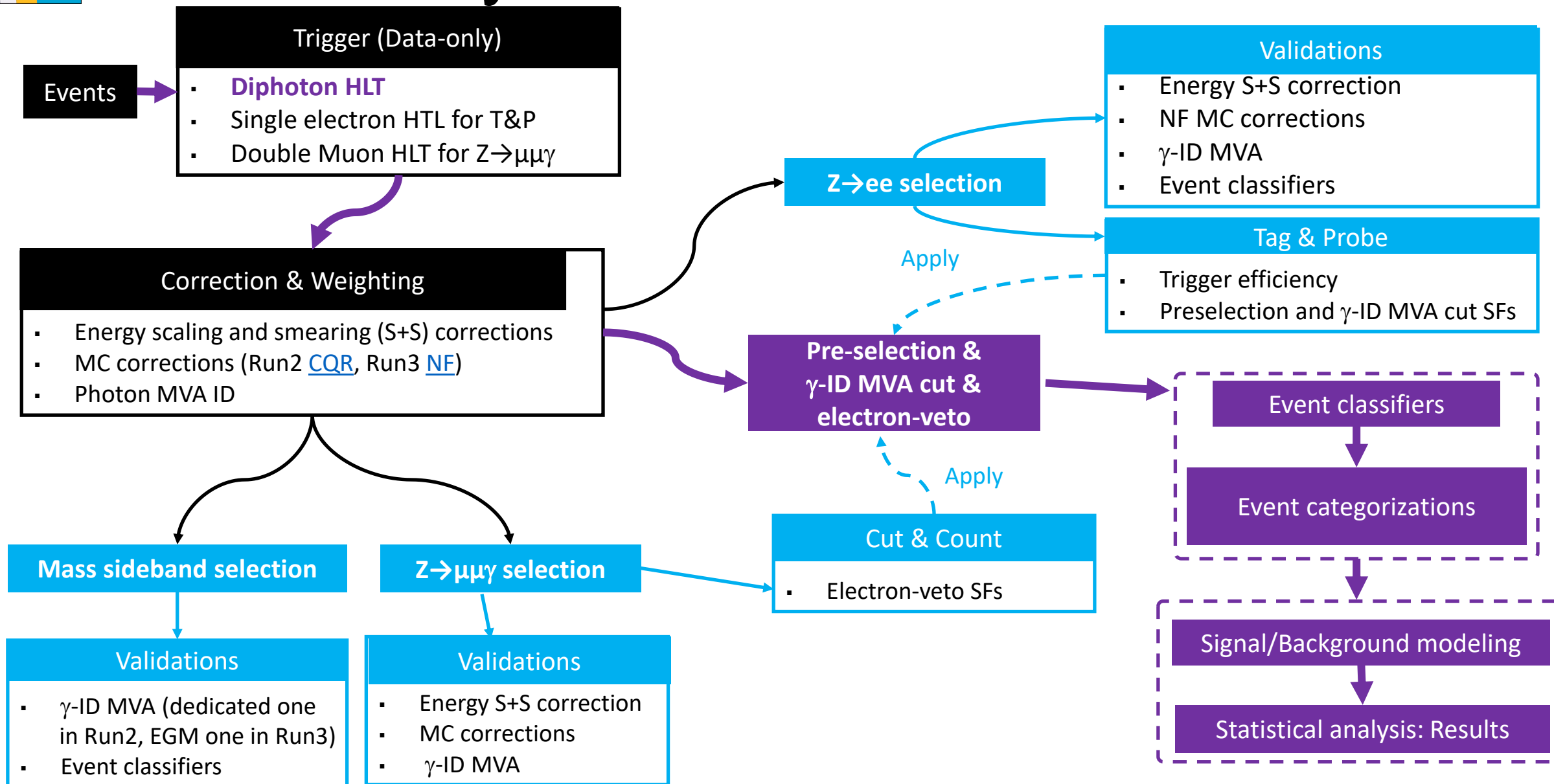


Bkg model derived from data, using the envelope method (discrete profiling method, 2015 JINST 10 P04015)

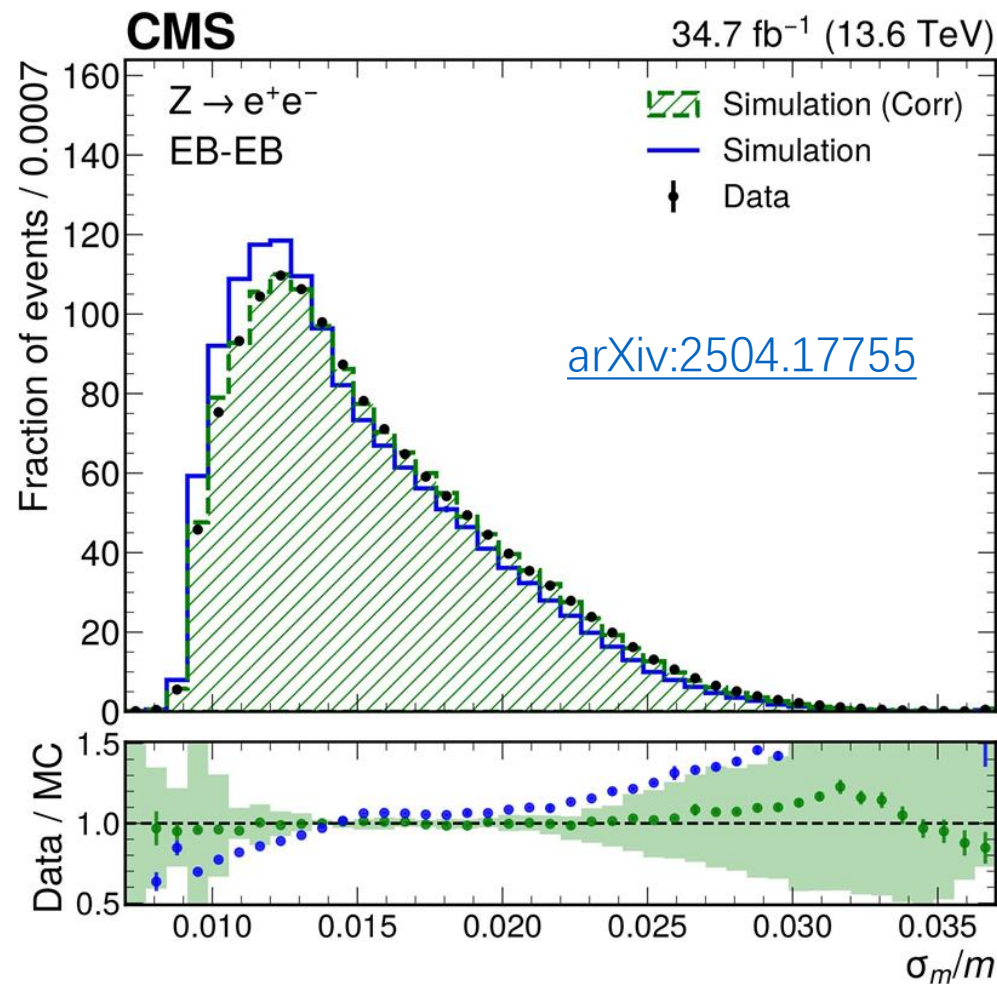


S+B fit to extract the signal simultaneously in all event classes

Analysis Workflow Overview



- **First $H \rightarrow \gamma\gamma$ analysis using CMS Run 3 data**
- Inclusive and differential measurements of the fiducial cross sections (XS) aim at **providing a set of model-independent results**
- Use of novel and innovative analysis techniques
 - ✓ **NN to improve γ energy resolution σ_E**
 - ✓ **Data/MC corrections** of γ shower shape, isolation and σ_E via normalizing flows → **reducing systematic uncertainties**
- **Three σ_m/m categories** are employed to improve the sensitivity: $[0, 0.0105)$, $[0.0105, 0.0130)$, and $[0.0130, \infty)$



Data-MC comparison before and after correcting σ_E , propagating to the mass resolution

Results of Run3 fiducial XS

➤ Fiducial volume

Run2

Observable	Selection
$p_T^{\gamma 1} / m_{\gamma\gamma}$	$> 1/3$
$p_T^{\gamma 2} / m_{\gamma\gamma}$	$> 1/4$
$\mathcal{I}_{\text{gen}}^{\gamma}$	$< 10 \text{ GeV}$
$ \eta^{\gamma} $	< 2.5

Run3 “geometric cut”

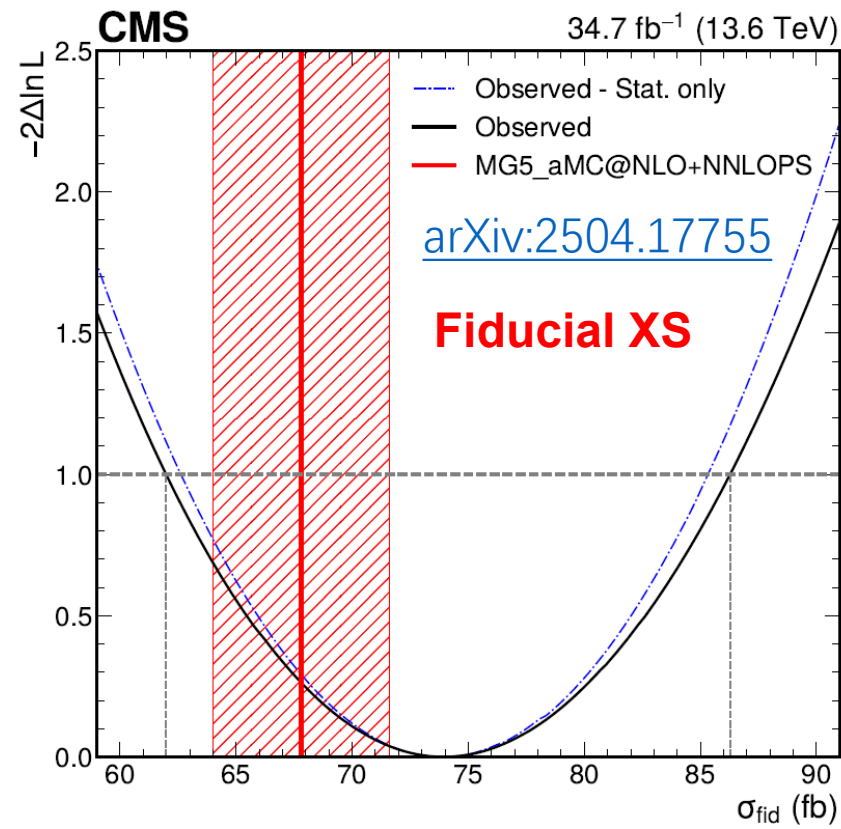
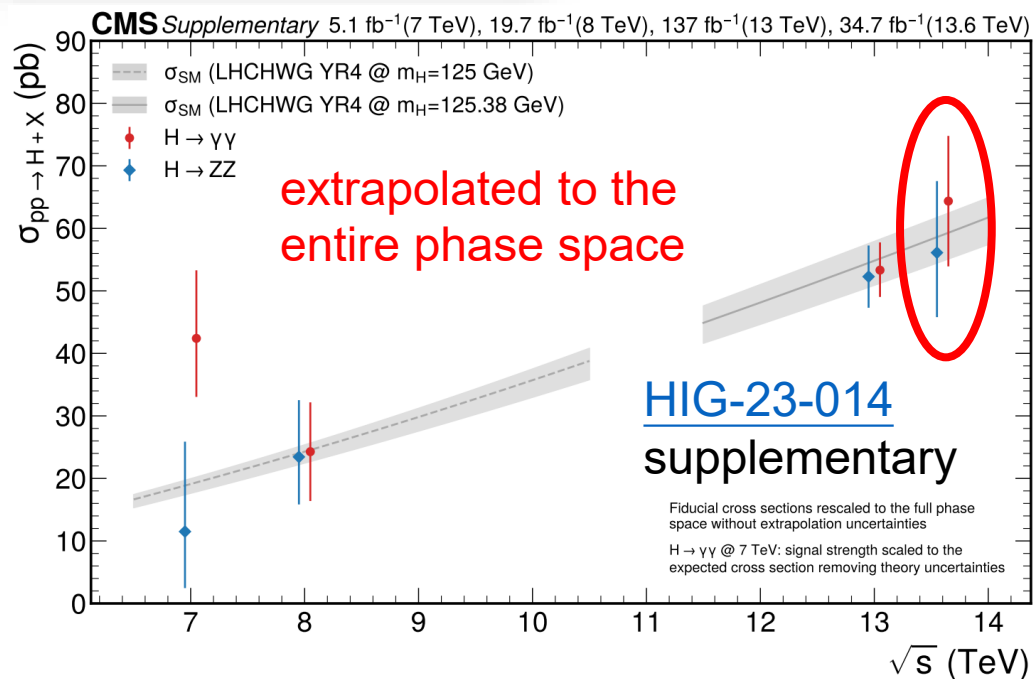
$$\sqrt{p_T^{\gamma 1} p_T^{\gamma 2}} / m_{\gamma\gamma} > 1/3$$

to improve perturbative convergence in the fiducial phase space [JHEP11(2021)220]

$$\sigma_{\text{fid}} = 74 \pm 12 \text{ fb} = 74 \pm 11 \text{ (stat)}^{+5}_{-4} \text{ (syst)} \text{ fb}$$

$$\text{Prediction: } 67.8 \pm 3.8 \text{ fb} = 67.8 \pm 2.6 \text{ (scales)} \pm 2.3 \text{ (PDF} + \alpha_s) \pm 1.4 \text{ (BR)} \text{ fb}$$

in agreement with the SM prediction



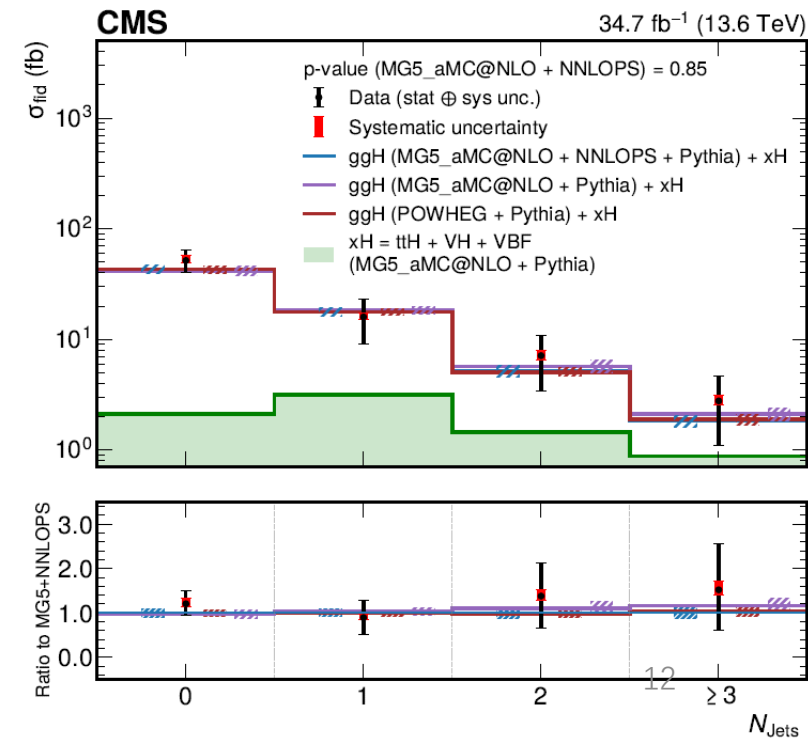
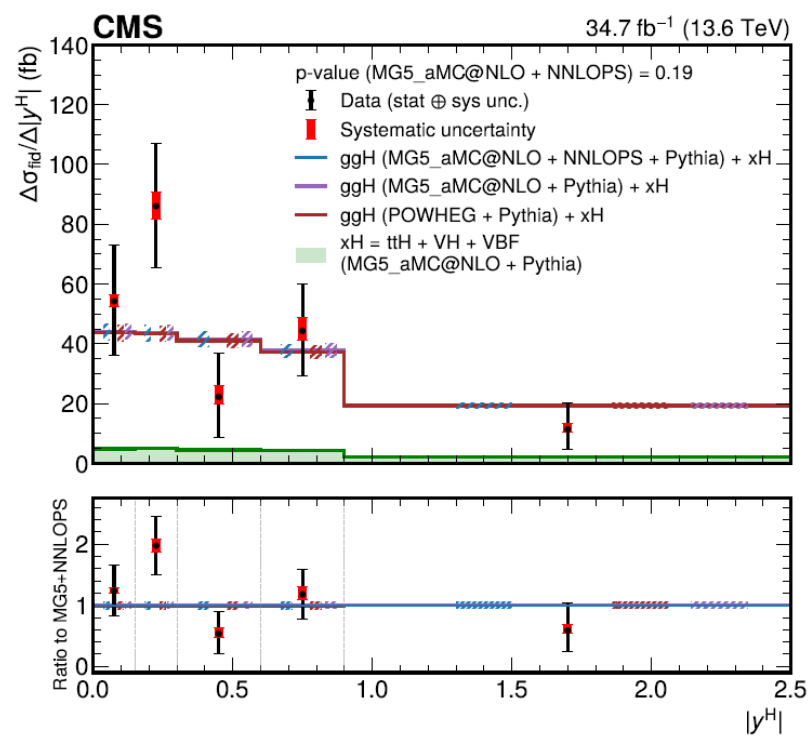
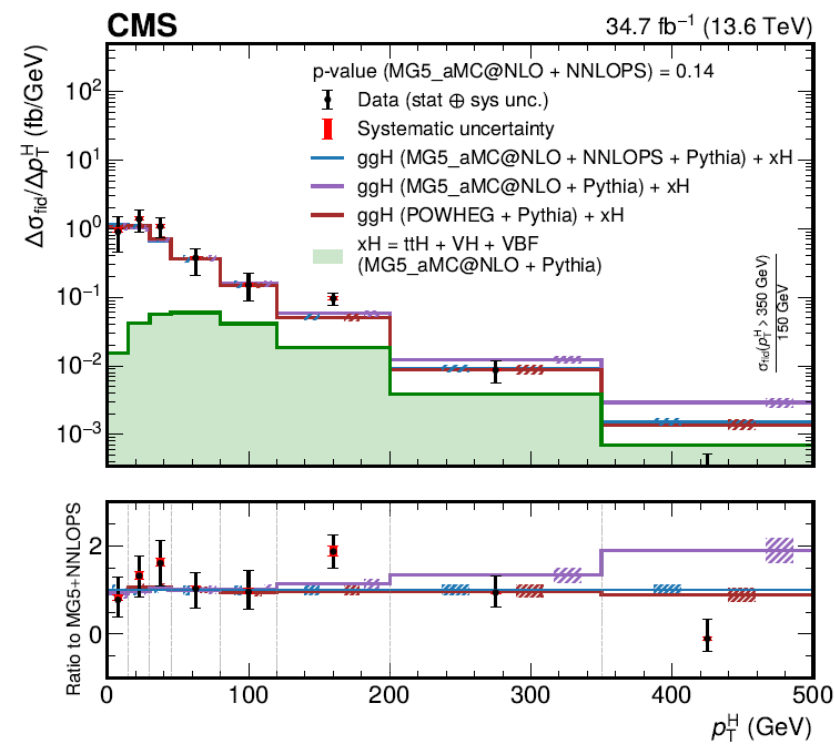
Run3 differential fiducial XS

➤ Fiducial XS measured as a function of each of the 4 observables

Observable	Bin boundaries								
p_T^H (GeV)	0	15	30	45	80	120	200	350	∞
$ y^H $	0	0.15	0.3	0.6	0.9	2.5			
N_{Jets}	0	1	2	3	∞				
p_T^{J1} (GeV)	0-jet	30	75	120	200	∞			

[arXiv:2504.17755](https://arxiv.org/abs/2504.17755)

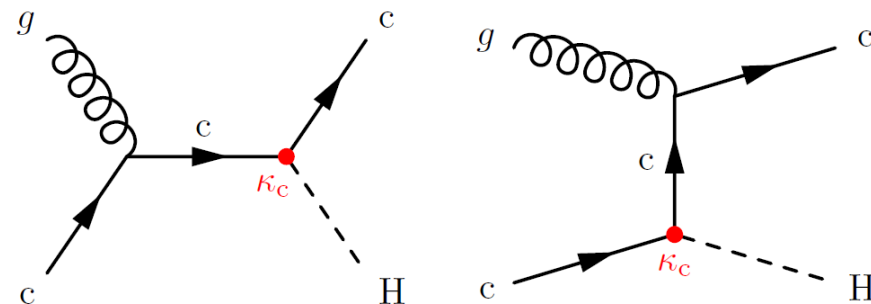
In agreement with the SM prediction within $\sim 1\text{-}2\sigma$ of the uncertainties



First search for cH , $H \rightarrow \gamma\gamma$

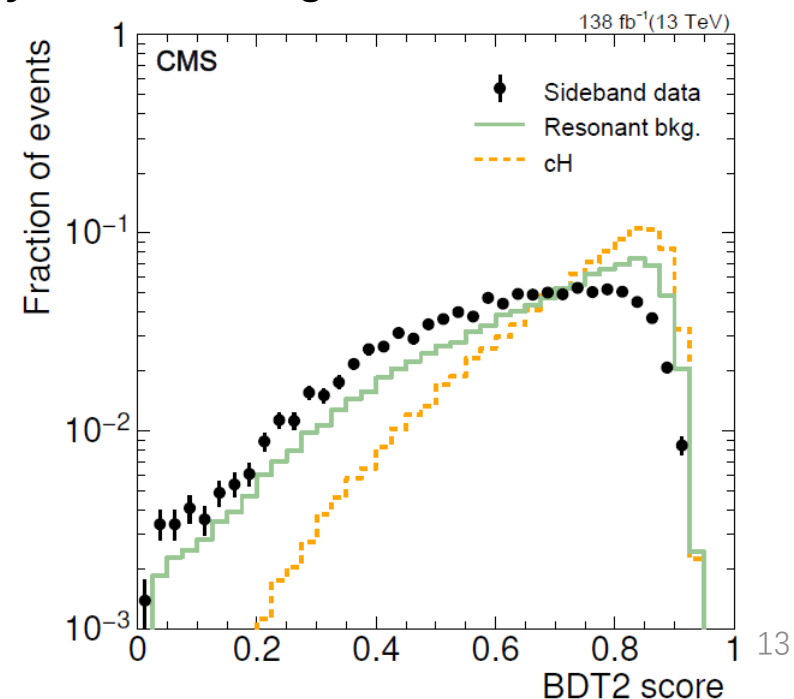
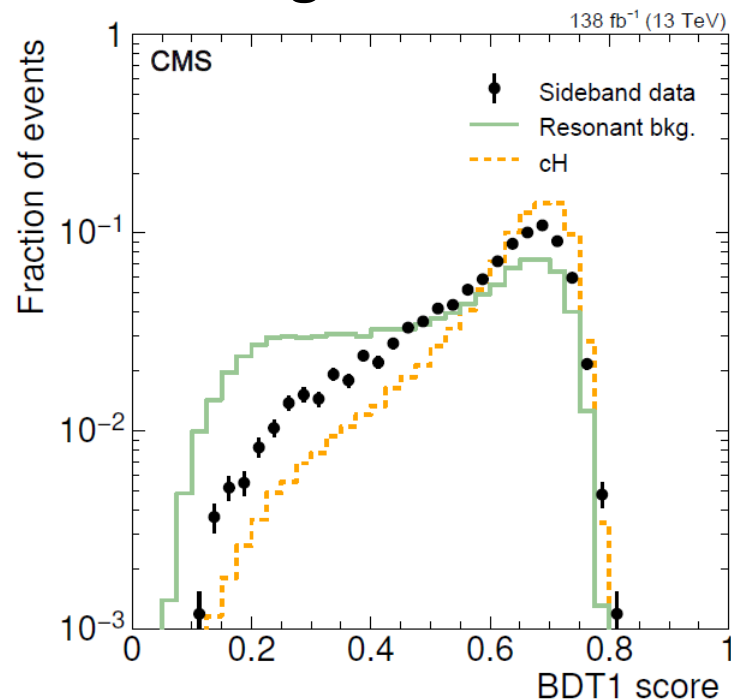
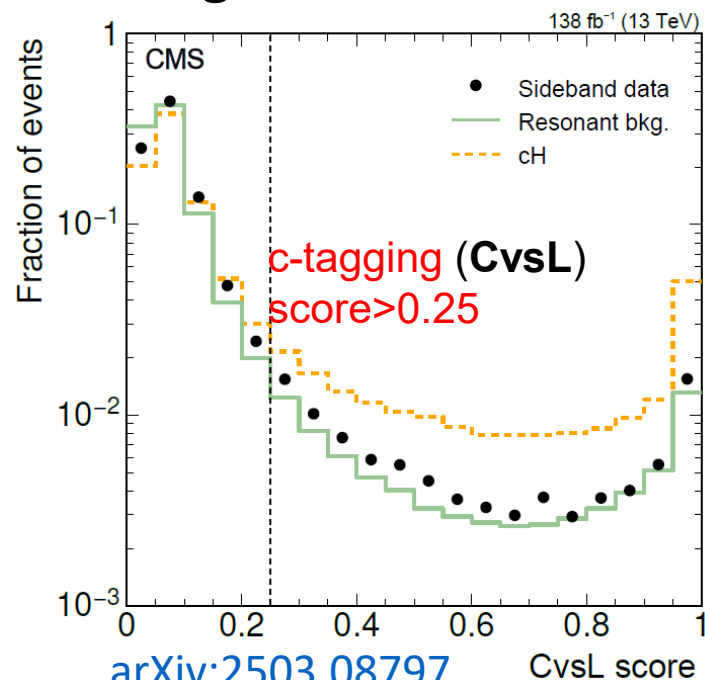
- Provide a unique opportunity to probe the **Higgs boson-charm quark coupling** in production of Higgs
- Jet with the largest p_T must be **c tagged** : CvsL score > 0.25

Tagger	CvsL
DeepJet	$\frac{P(c)}{P(c)+P(uds)+P(g)}$



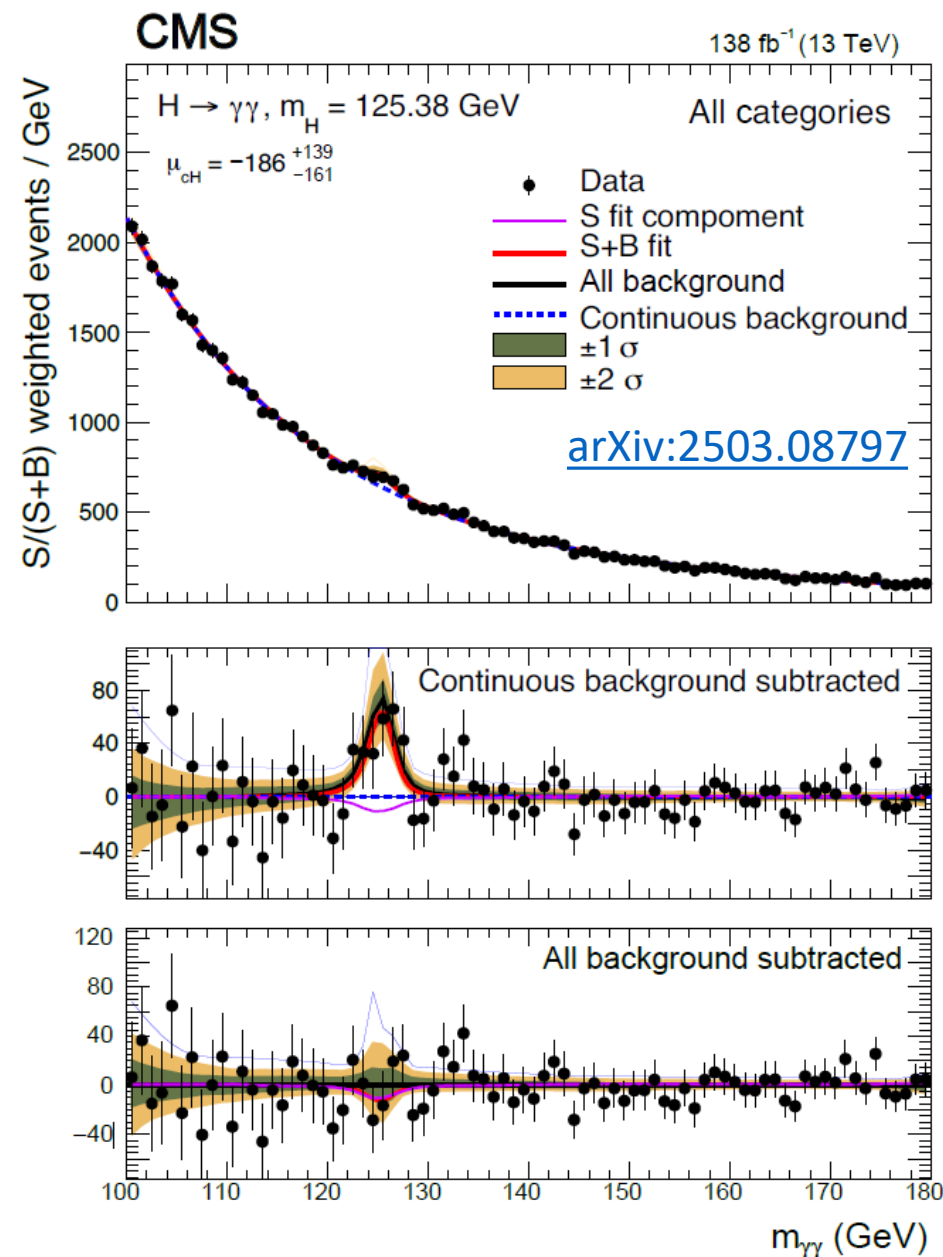
- **Two BDT classifiers** to distinguish cH and ggH , to distinguish cH and the **continuous bkg**

Events are divided into **9 categories** for each year, according to BDT1 and BDT2 scores



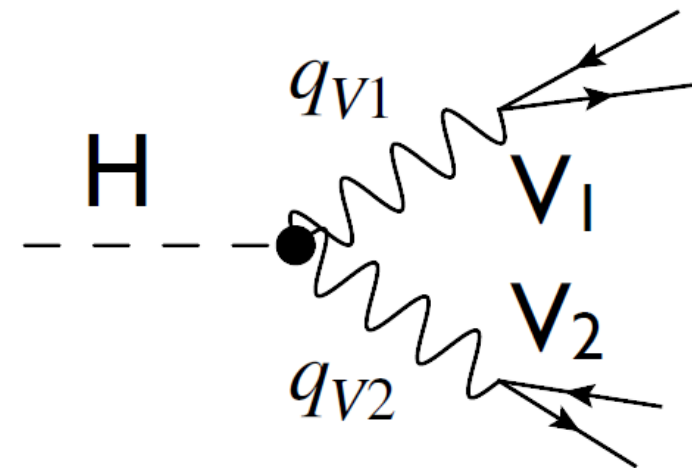
Results of search for cH , $H \rightarrow \gamma\gamma$

- Upper limits on the cH signal strength < 243 (355) $\times \sigma_{SM}$ obs. (exp.) at 95% CL
- Constraints on H-c quark coupling modifier $|\kappa_c| < 38.1$ ($|\kappa_c| < 72.5$) obs. (exp.) at 95% CL
- Dominated by the **statistical uncertainty of data**, sub-dominated by **theoretical uncertainties** on cH signal and resonant bkg



Anomalous Higgs Interactions

- Higgs boson confirmed to be spin-0, and **consistent with CP++** since Run1
- Pure CP-odd state excluded \neq CP-even state
- Look for **BSM contributions** in the HVV, Hgg amplitudes



$$V_i = W, Z, \gamma, g$$

$$A(HV_1V_2) = \frac{1}{v} \left[\boxed{a_1^{VV}} + \boxed{\frac{\kappa_1^{VV} q_{V1}^2 + \kappa_2^{VV} q_{V2}^2 + \kappa_3^{VV} (q_{V1} + q_{V2})^2}{(\Lambda_1^{VV})^2} + \frac{\kappa_3^{VV} (q_{V1} + q_{V2})^2}{(\Lambda_Q^{VV})^2}} \right] m_{V1}^2 \epsilon_{V1}^* \epsilon_{V2}^* + \boxed{\frac{1}{v} a_2^{VV} f_{\mu\nu}^{*(1)} f^{*(2),\mu\nu}} + \boxed{\frac{1}{v} a_3^{VV} f_{\mu\nu}^{*(1)} \tilde{f}^{*(2),\mu\nu}}$$

a_1 : SM Dim-6 BSM operators at a scale $\Lambda \gg \Lambda_{\text{EWK}}$ a_2 : CP even BSM a_3 : CP odd BSM

Anomalous couplings with $H \rightarrow \gamma\gamma$

- **VBF+VH** to probe anomalous **HVV** interactions ($f_{a2}, f_{a3}, f_{\Lambda 1}, f_{\Lambda 1}^{Z\gamma}$), **ggH** to probe anomalous **Hgg** interactions ($f_{a3}^{ggH}, f_{CP}^{Htt}$) in the top quark dominated loop

*ttH already in [PRL 125 \(2020\) 061801](#)

fractional contribution of each anomalous Higgs boson coupling to the total cross section of a process

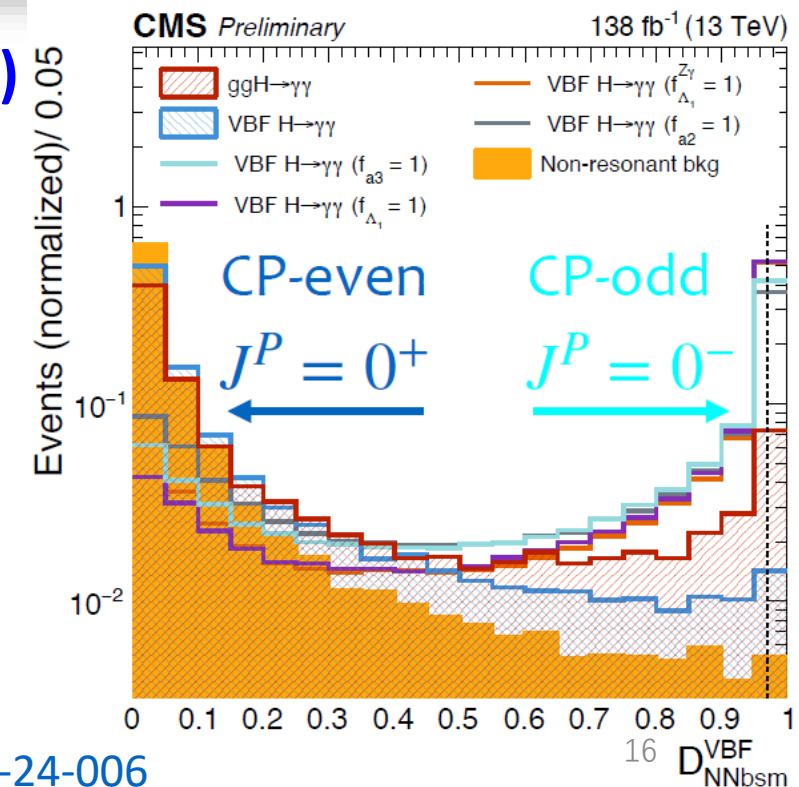
$$f_{ai} = \frac{|a_i|^2 \sigma_i}{|a_1|^2 \sigma_1 + |a_2|^2 \sigma_2 + |a_3|^2 \sigma_3 + \tilde{\sigma}_{\Lambda 1} / (\Lambda_1)^2 + \tilde{\sigma}_{\Lambda 1}^{Z\gamma} / (\Lambda_1^{Z\gamma})^2} \times \text{sgn} \left(\frac{a_i}{a_1} \right)$$

$$f_{a3}^{ggH} = \frac{|a_3^{gg}|^2}{|a_2^{gg}|^2 + |a_3^{gg}|^2} \times \text{sgn} \left(\frac{a_3^{gg}}{a_2^{gg}} \right) \quad |f_{CP}^{Htt}| = \left(1 + 2.38 \left[\frac{1}{|f_{a3}^{ggH}|} - 1 \right] \right)^{-1}$$

- **Discriminants** are defined using **several machine learning (ML)** algorithms and the **matrix element likelihood** approach (*)

- ✓ To enhance the separations between **SM Higgs and anomalous coupling signal hypotheses, SM Higgs and bkg**
- ✓ For **event categorizations**

VBF+VH	$\mathcal{D}_{\text{NNBSM}}^{\text{VBF}}$ and $\mathcal{D}_{\text{BSM}}^{\text{VHhad}}$	$\mathcal{D}_{\text{NNbkg}}^{\text{VBF}}$ and $\mathcal{D}_{\text{bkg}}^{\text{VHhad}}$
	$\mathcal{D}_{\text{BSM}}^{\text{VHMET}}, \mathcal{D}_{\text{BSM}}^{\text{WHlep}}, \text{ and } \mathcal{D}_{\text{BSM}}^{\text{ZHlep}}$	$\mathcal{D}_{\text{STXS}}^{\text{VHMET}}, \mathcal{D}_{\text{STXS}}^{\text{WHlep}}, \text{ and } \mathcal{D}_{\text{STXS}}^{\text{ZHlep}}$
ggH	$\mathcal{D}_{0-}^{\text{ggH}}$ and $\mathcal{D}_{\text{CP}}^{\text{ggH}}$	$\mathcal{D}_{\text{BSM}}^{\text{ggH}+2\text{jets}}, \mathcal{D}_{\text{STXS}}^{\text{ggH}}, \text{ and } \mathcal{D}_{\text{bkg}}^{\text{ggH}+2\text{jets}}$



* [Phys. Rev. Lett. 110 \(2013\) 081803](#)

H $\rightarrow\gamma\gamma$ AC: HVV coupling parameters

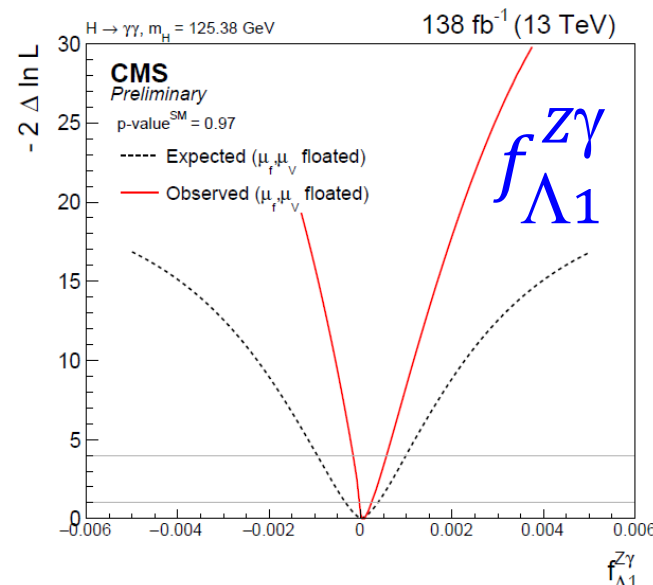
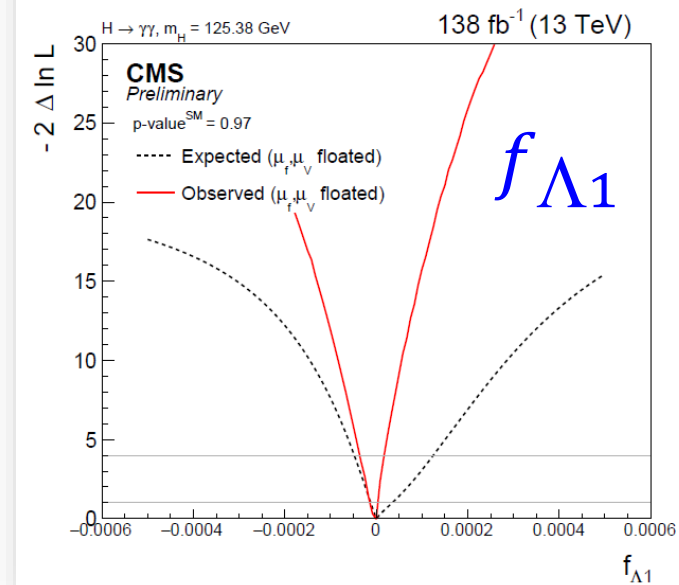
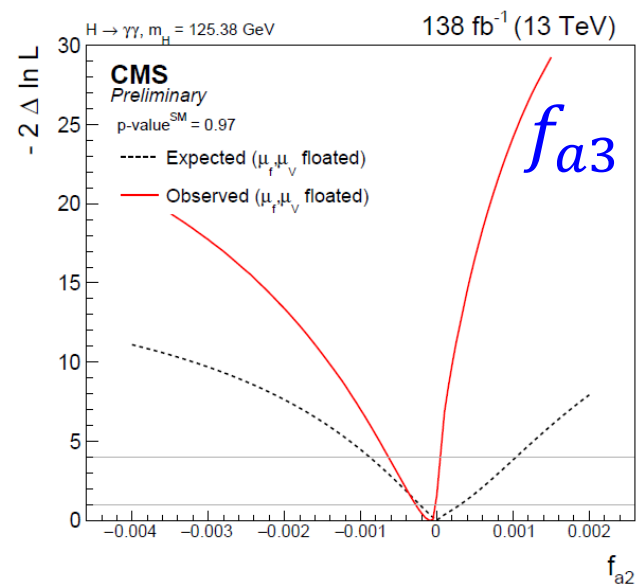
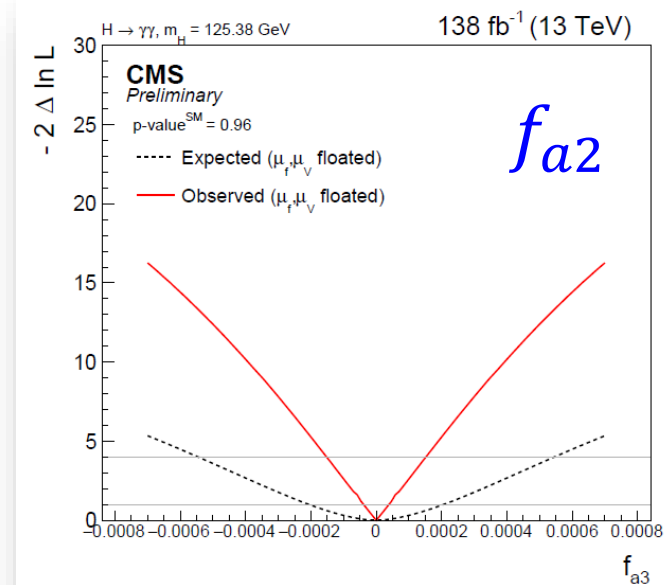
Very new: released
for EPS2025 (July)

68% CL intervals on HVV AC parameters

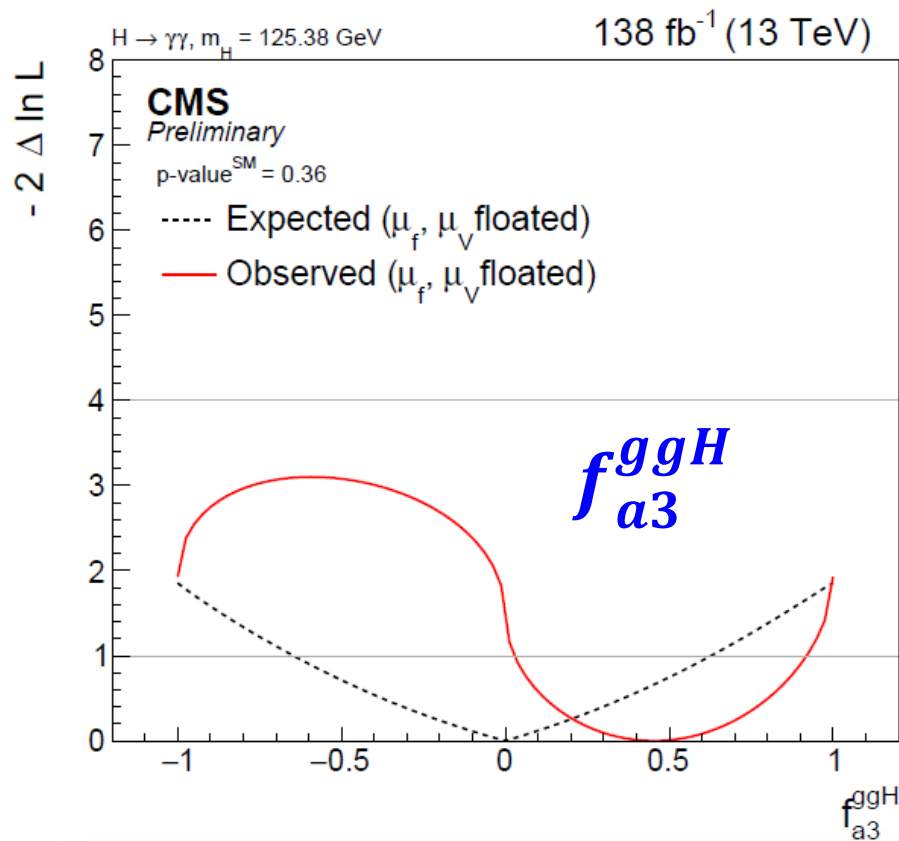
Parameter	Expected/(10 ⁻⁴) H $\rightarrow \gamma\gamma$ (68% CL)	Observed/(10 ⁻⁴) H $\rightarrow \gamma\gamma$ (68% CL)	Expected/(10 ⁻⁴) H $\rightarrow 4\ell + H \rightarrow \tau^+\tau^-$ (68% CL)
f_{a3}	$0.0^{+2.1}_{-2.1}$	$0.00^{+0.39}_{-0.39}$	$[-0.5, 0.5]$
f_{a2}	$0.0^{+3.1}_{-2.3}$	$-0.81^{+0.65}_{-2.0}$	$[-4, 5]$
$f_{\Lambda 1}$	$0.0^{+0.35}_{-0.12}$	$-0.014^{+0.032}_{-0.14}$	$[-0.4, 1.1]$
$f_{\Lambda 1}^{Z\gamma}$	$0.0^{+3.7}_{-3.3}$	$0.83^{+1.5}_{-0.92}$	$[-10, 10]$

➤ **Compatible wrt SM prediction**
($f_{ai}=0$)

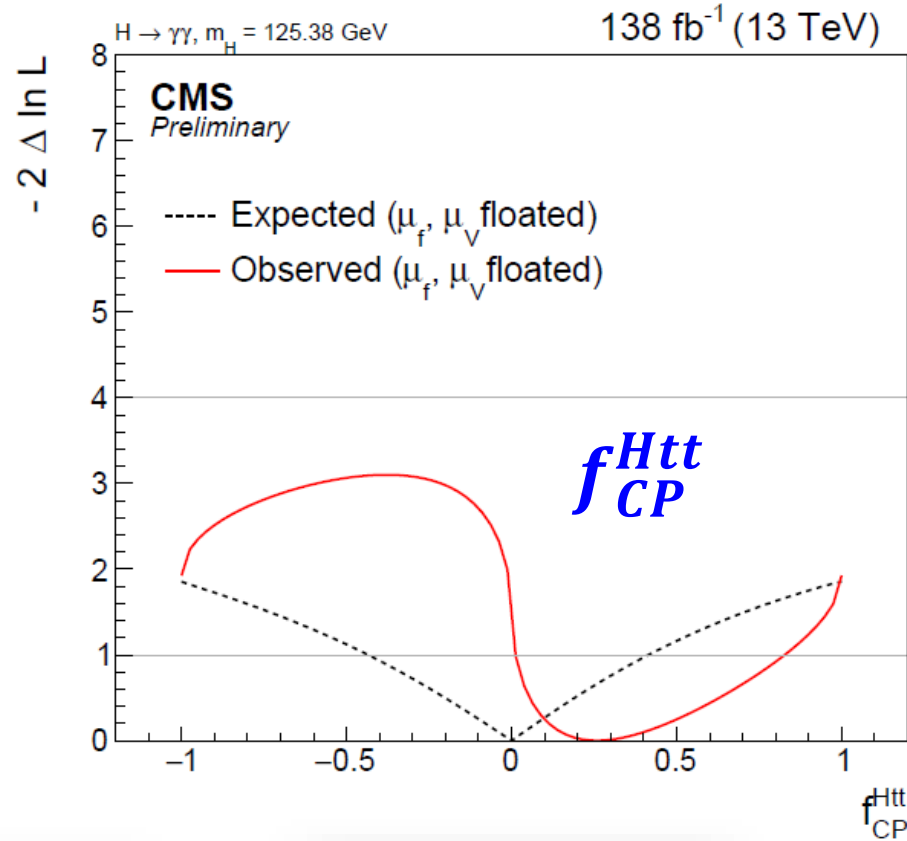
➤ **These represent some of the**
most stringent limits to date



H $\rightarrow\gamma\gamma$ AC: Hgg coupling parameters



$$f_{a3}^{ggH} = 0.45^{+0.46}_{-0.42} \text{ (stat.) } ^{+0.10}_{-0.08} \text{ (syst.)}$$



$$f_{CP}^{Htt} = 0.26^{+0.57}_{-0.25}$$

Very new: released
for EPS2025 (July)

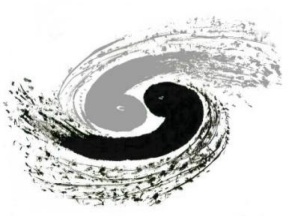
**Results consistent
with SM expectations**

As systematic uncertainties largely cancel in ratios, all measurements are currently **limited by the statistical precision** and are expected to improve with additional LHC data

$$f_{a3}^{ggH} = \frac{|a_3^{gg}|^2}{|a_2^{gg}|^2 + |a_3^{gg}|^2} \times \text{sgn} \left(\frac{a_3^{gg}}{a_2^{gg}} \right)$$

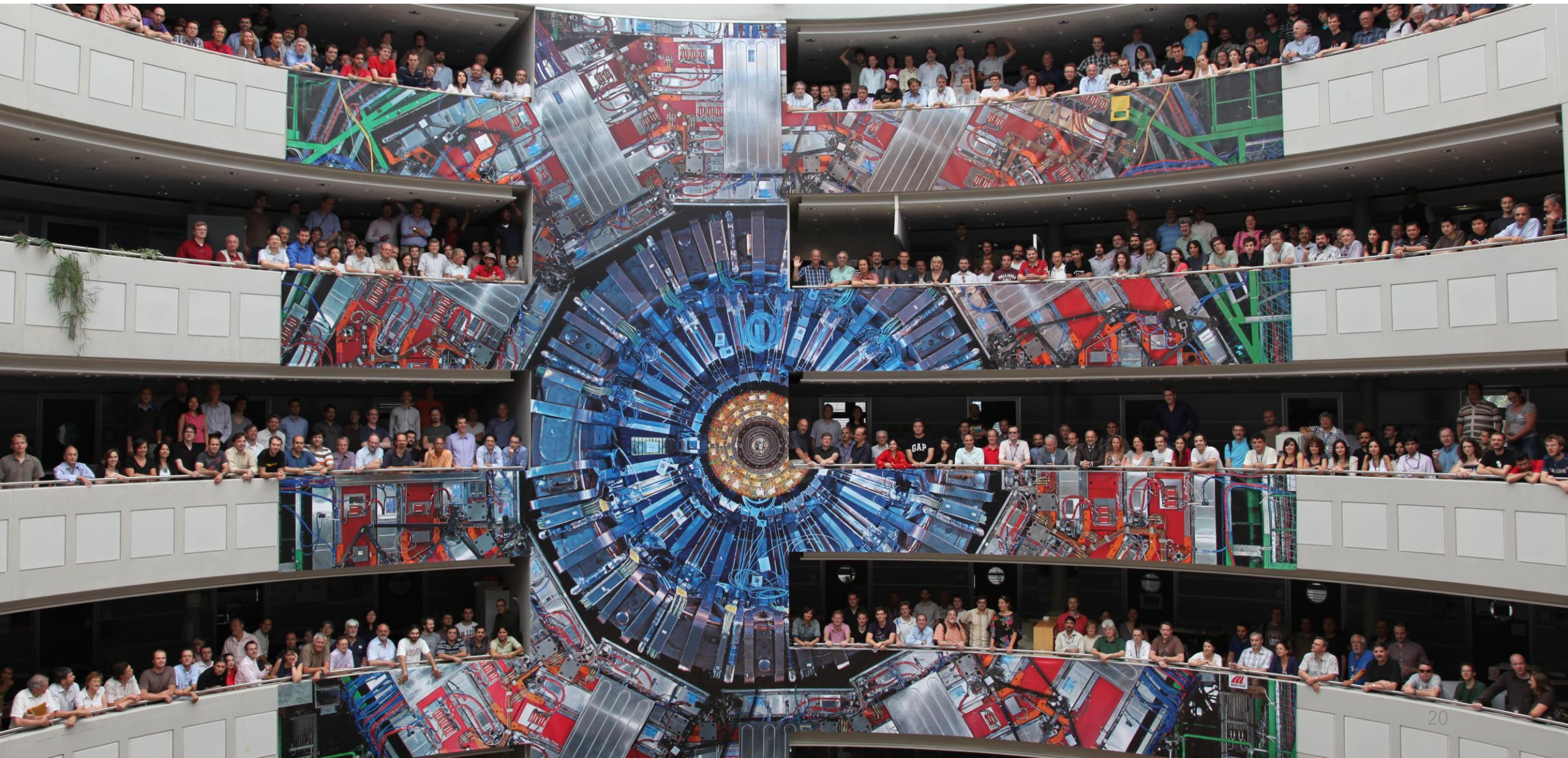


Summary



- **Latest results** of Higgs boson property measurements with $H \rightarrow \gamma\gamma$ are presented
 - ✓ Inclusive and differential **fiducial cross section** with Run3 (2022) data
 - ✓ First search for **$H+c$ ($H \rightarrow \gamma\gamma$)** at LHC with Run2 data to probe Higgs-charm coupling
 - ✓ Probing possible **anomalous couplings** of the Higgs boson to vector bosons and fermions with Run2 data
- **All measured results are consistent with Standard Model prediction**
- **More Run2** ($H \rightarrow \gamma\gamma$ Higgs mass and width, $HHH \rightarrow 4b2\gamma$, ...) **and Run3 results** (STXS, $HH \rightarrow bb\gamma\gamma$, ...) **are coming ... please stay tuned!**

Thanks for your attention!



Backup

H $\rightarrow\gamma\gamma$ Run3 cross sections

➤ Fiducial volume

Run2

Observable	Selection
$p_T^{\gamma 1}/m_{\gamma\gamma}$	$>1/3$
$p_T^{\gamma 2}/m_{\gamma\gamma}$	$>1/4$
$\mathcal{I}_{\text{gen}}^{\gamma}$	<10 GeV
$ \eta^{\gamma} $	<2.5

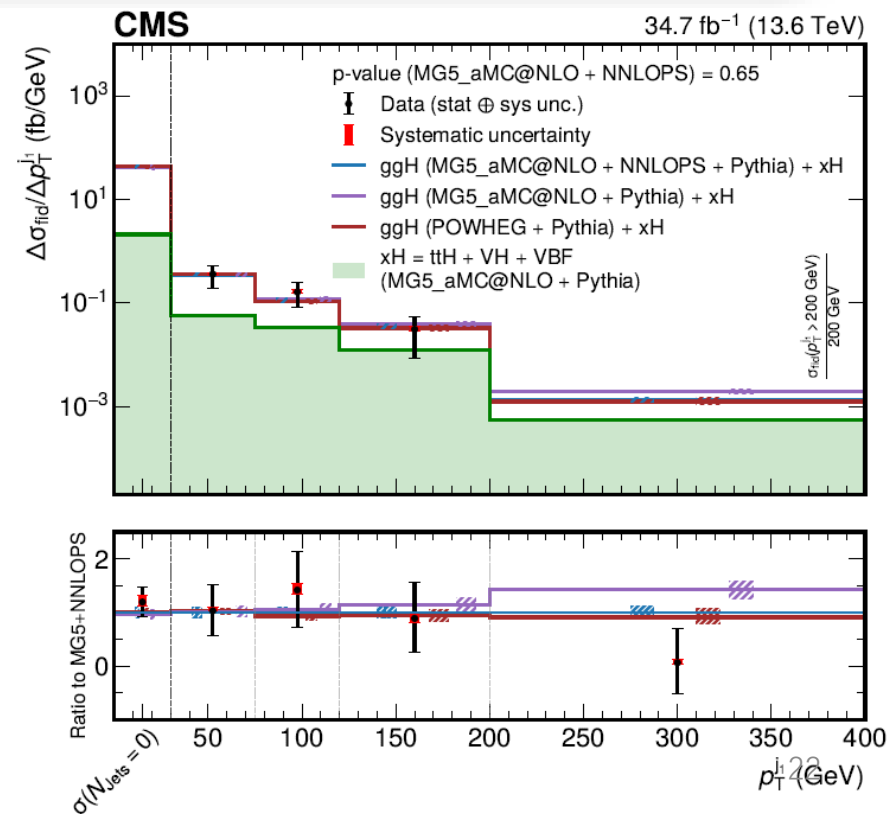
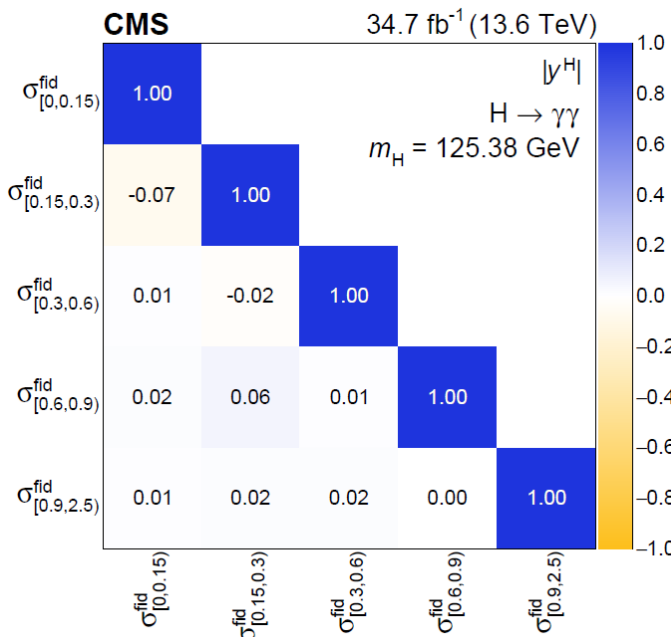
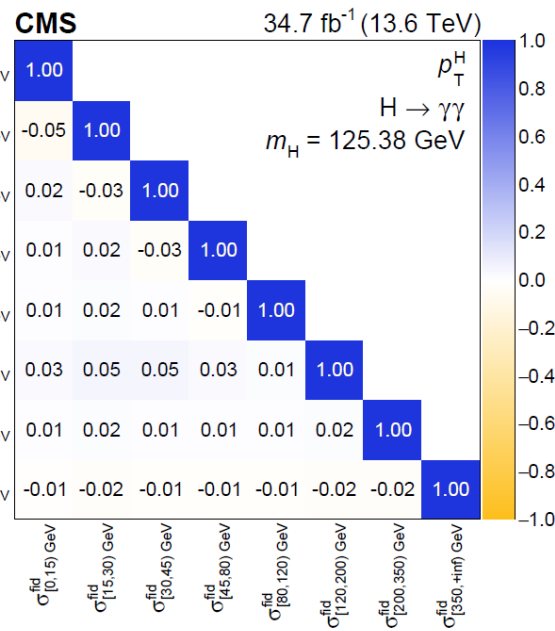
Run3 “geometric cut”

$$\sqrt{p_T^{\gamma 1} p_T^{\gamma 2}}/m_{\gamma\gamma} > 1/3$$

Efficiency of these criteria, as determined from simulation, is $\approx 51.8\%$ with Run2 volume and $\approx 50.6\%$ with Run3 “geometric cut”

Systematic uncertainty

Systematic uncertainty	Impact in %
Category migration from energy resolution	$+3.5/-4.2$
Photon energy scale and resolution group	$+3.4/-2.8$
Integrated luminosity	± 1.4
Photon preselection efficiency	± 1.4
Material budget	$+1.3/-1.2$
Photon identification efficiency	± 1.0
Pileup reweighting	± 0.8



Search for cH , $H \rightarrow \gamma\gamma$

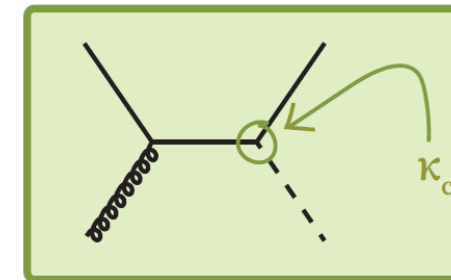
Table 1: Number of expected signal cH ($H \rightarrow \gamma\gamma$), resonant background and continuous background events, as well as the resulting signal-over-background ratio (S/B) in the diphoton mass window $[122.88, 127.88]$ GeV for all categories. For each category, the event yields for the three years are summed. The fraction of different production processes contributing to the resonant background (ggH, $t\bar{t}H$, VBF, VH, and bH) is also reported.

Category	Signal	Resonant background						Continuous bkg. ($\times 10^3$)	S/B ($\times 10^{-5}$)
	cH	ggH	$t\bar{t}H$	VBF	VH	bH	Total		
Tag0	0.013	84%	<0.1%	5.3%	3.4%	7.5%	2.4	0.50	2.6
Tag1	0.016	79%	0.33%	7.3%	6.3%	7.3%	3.3	1.5	1.0
Tag2	0.0072	72%	4.0%	8.3%	9.1%	6.4%	1.8	7.4	0.10
Tag3	0.0034	72%	<0.1%	16%	5.9%	5.6%	1.3	0.17	2.0
Tag4	0.0087	68%	1.2%	16%	9.9%	4.9%	3.5	0.96	0.90
Tag5	0.0094	54%	15%	15%	14%	3.6%	5.1	9.9	0.10
Tag6	0.00029	42%	1.9%	43%	12%	1.5%	0.52	0.019	1.5
Tag7	0.00095	43%	14%	25%	17%	1.3%	1.8	0.16	0.59
Tag8	0.0017	36%	32%	15%	17%	1.1%	3.3	1.9	0.087
All	0.060	61%	9.4%	14%	11%	4.5%	23	23	0.27

Table 2: Impacts of several uncertainty groups divided by the total uncertainty in the signal strength measurement.

Uncertainty group	Fraction of total impact
Statistical	66%
Theoretical in the cH signal	38%
Theoretical in the resonant background	59%
Experimental in the yields	27%
Experimental in the mass shapes	<1%
Integrated luminosity	<1%

$pp \rightarrow H + c$



HIG-23-010

Sensitive to κ_c in production of Higgs

Strong constraints on κ_c at 95% CL!

$t\bar{t}H(c\bar{c}) + VH(c\bar{c})$

$$\kappa_c < 3.5$$

$H(\gamma\gamma)+c$

$$\kappa_c < 31.8$$

$H(4l)+X$

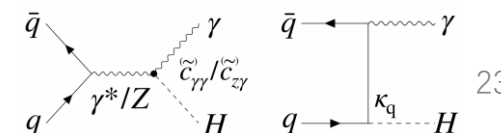
$$-4.0 < \kappa_c < 3.4$$

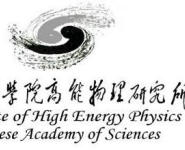
HIG-24-018: $t\bar{t}H(cc)$

[arXiv:2503.08797](https://arxiv.org/abs/2503.08797)

HIG-23-011:

$H(ZZ/bb)+\gamma$ production with the boosted topology

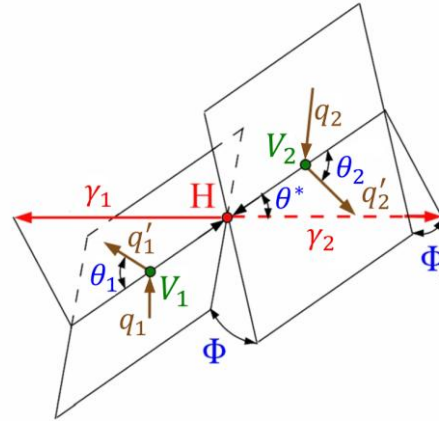




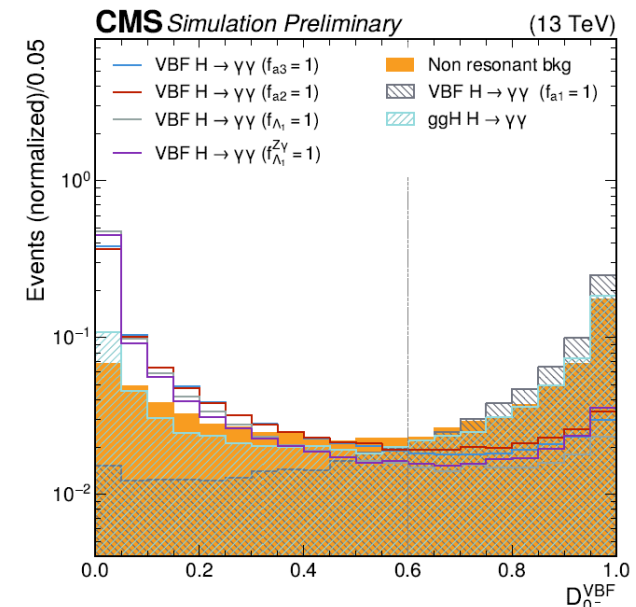
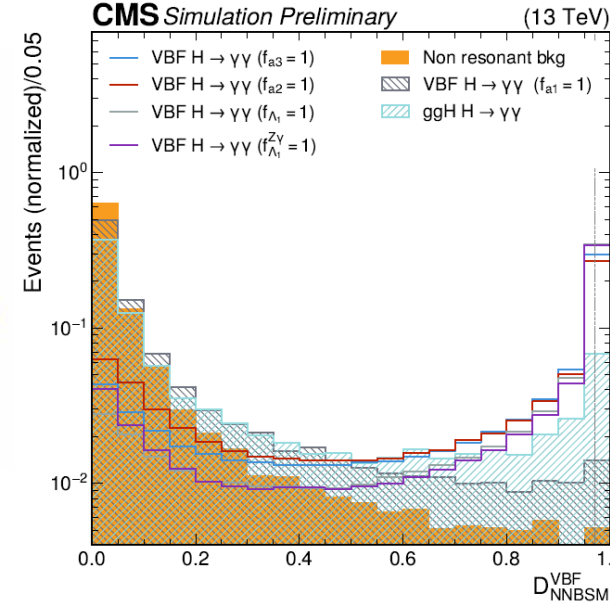
H $\rightarrow\gamma\gamma$ AC : VBF, VH

Table 2: List of discriminants for separating anomalous couplings from the SM contribution in the HVV analysis. The third column indicates the targeted discrimination for that specific observable. Discriminants in this table are only used for event categorization.

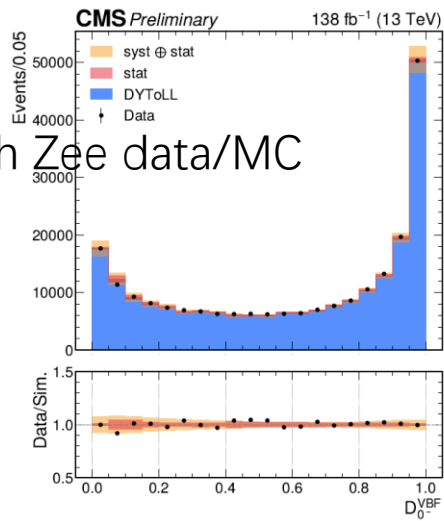
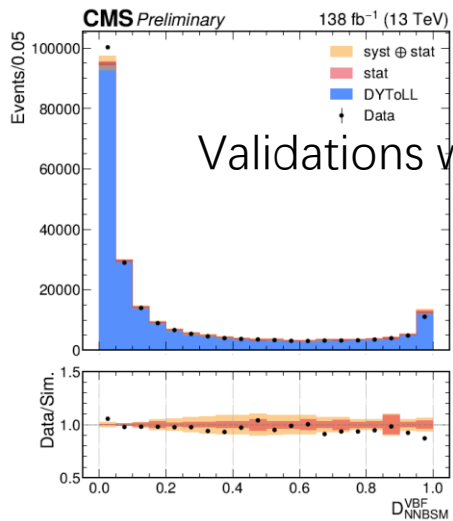
Production mode	Discriminant	Main goal
VBF	$\mathcal{D}_{0-}^{\text{VBF}}$	separate between CP-even, CP-odd and mixed CP scenarios
VBF	$\mathcal{D}_{\text{NNbkg}}^{\text{VBF}}$	separate H signal from non-resonant backgrounds
VBF	$\mathcal{D}_{\text{NNBSM}}^{\text{VBF}}$	separate between SM H and several BSM H scenarios
V(had)H	$\mathcal{D}_{\text{bkg}}^{\text{VHhad}}$	separate H signal from non-resonant backgrounds
V(had)H	$\mathcal{D}_{\text{BSM}}^{\text{VHhad}}$	separate between SM H and several BSM H scenarios
W($\ell\nu$)H	$\mathcal{D}_{\text{STXS}}^{\text{WHlep}}$	separate H signal from non-resonant backgrounds
W($\ell\nu$)H	$\mathcal{D}_{\text{BSM}}^{\text{WHlep}}$	separate H signal from several BSM H scenarios
Z($\ell\ell$)H	$\mathcal{D}_{\text{STXS}}^{\text{ZHlep}}$	separate H signal from non-resonant backgrounds
Z($\ell\ell$)H	$\mathcal{D}_{\text{BSM}}^{\text{ZHlep}}$	separate H signal from several BSM H scenarios
Z($\nu\nu$)H	$\mathcal{D}_{\text{STXS}}^{\text{VHMET}}$	separate H signal from non-resonant backgrounds
Z($\nu\nu$)H	$\mathcal{D}_{\text{BSM}}^{\text{VHMET}}$	separate H signal from several BSM H scenarios



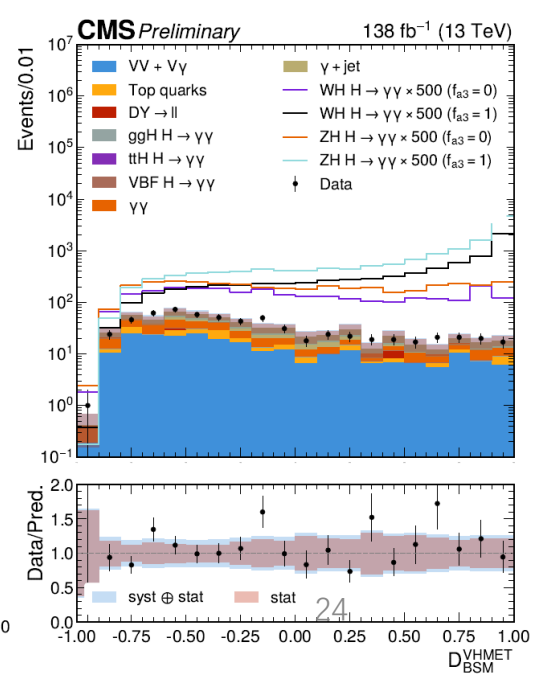
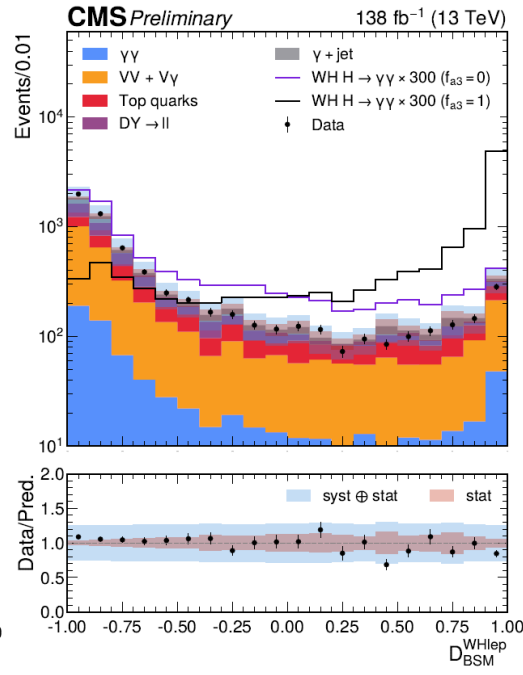
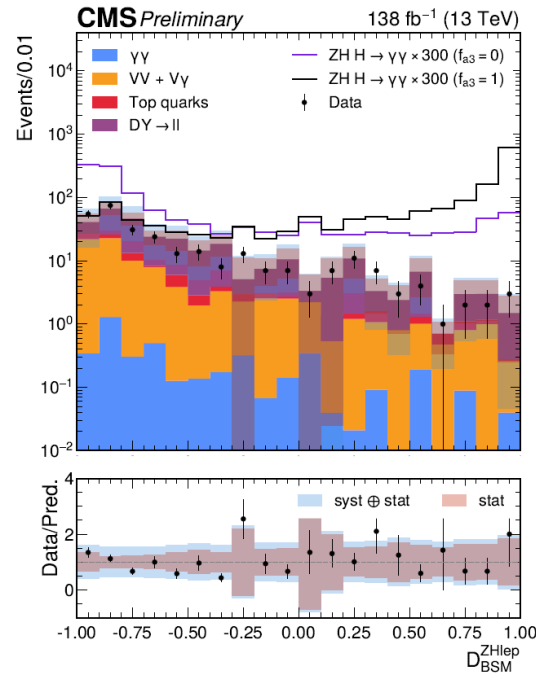
diphoton system + additional final-state particles



[HIG-24-006](#)



Validations with Zee data/MC



H $\rightarrow\gamma\gamma$ AC : VBF, VH

Table 4: Definition of the VBF categories based on the values of the discriminants $\mathcal{D}_{\text{NNbkg}}^{\text{VBF}}$, $\mathcal{D}_{0-}^{\text{VBF}}$ and $\mathcal{D}_{\text{NNBSM}}^{\text{VBF}}$.

Analysis categories	$\mathcal{D}_{\text{NNbkg}}^{\text{VBF}}$	$\mathcal{D}_{0-}^{\text{VBF}}$	$\mathcal{D}_{\text{NNBSM}}^{\text{VBF}}$
ggH-like Tag0	> 0.05	> 0.6	< 0.97
ggH-like Tag1	> 0.05	< 0.6	< 0.97
qqH BSM-like Tag0	< 0.05	< 0.6	> 0.97
qqH BSM-like Tag1	< 0.05	< 0.6	< 0.97
qqH SM-like Tag0	< 0.05	> 0.6	< 0.97

Table 5: The expected number of signal events in the case of SM H with $m_H = 125$ GeV in analysis categories targeting VBF associated production, shown for an integrated luminosity of 138 fb^{-1} . The fraction of the total number of events arising from the VBF production mode in each analysis category is provided. Entries with values less than 0.1% are not shown. The σ_{eff} , defined as the smallest interval containing 68.3% of the $m_{\gamma\gamma}$ distribution, is listed for each analysis category. The final column shows the expected ratio of signal to signal-plus-background, $S/(S+B)$, where S and B are the numbers of expected signal and background events in a $\pm 1\sigma_{\text{eff}}$ window centered on m_H .

Analysis categories	H(125) expected signal			
	yield	qqH	σ_{eff} (GeV)	$S/(S+B)$
ggH-like Tag0	118.9	44%	1.86	0.07
ggH-like Tag1	64.2	23%	1.71	0.05
qqH BSM-like Tag0	11.3	12%	1.55	0.51
qqH BSM-like Tag1	30.8	59%	1.67	0.45
qqH SM-like Tag0	79.1	75%	1.86	0.37

[HIG-24-006](#)

Table 6: Definition of the V(had)H categories (i.e. VH events where the vector boson decays hadronically) based on the values of the discriminants $\mathcal{D}_{\text{bkg}}^{\text{VHhad}}$ and $\mathcal{D}_{\text{BSM}}^{\text{VHhad}}$.

Analysis categories	$\mathcal{D}_{\text{bkg}}^{\text{VHhad}}$	$\mathcal{D}_{\text{BSM}}^{\text{VHhad}}$
V(had)H SM Tag0	< 0.08	< 0.56
V(had)H SM Tag1	$0.08 < \mathcal{D}_{\text{bkg}}^{\text{VHhad}} < 0.25$	< 0.45
V(had)H SM Tag2	$0.25 < \mathcal{D}_{\text{bkg}}^{\text{VHhad}} < 0.54$	< 0.29
V(had)H BSM Tag0	< 0.066	> 0.89
V(had)H BSM Tag1 (excluding cat. V(had)H BSM Tag0)	< 1.0	> 0.75

Table 7: The expected number of signal events in the case of SM H with $m_H = 125$ GeV in analysis categories targeting VH associated production in which the vector boson decays hadronically, shown for an integrated luminosity of 138 fb^{-1} . The fraction of the total number of events arising from the VH production mode in each analysis category is provided. Entries with values less than 0.1% are not shown. The σ_{eff} , defined as the smallest interval containing 68.3% of the $m_{\gamma\gamma}$ distribution, is listed for each analysis category. The final column shows the expected ratio of signal to signal-plus-background, $S/(S+B)$, where S and B are the numbers of expected signal and background events in a $\pm 1\sigma_{\text{eff}}$ window centered on m_H .

Analysis categories	H(125) expected signal			
	yield	VH	σ_{eff} (GeV)	$S/(S+B)$
V(had)H SM Tag0	16.6	4%	1.69	0.13
V(had)H SM Tag1	37.6	34%	1.70	0.07
V(had)H SM Tag2	100.5	16%	1.63	0.05
V(had)H BSM Tag0	4.41	13%	1.72	0.30
V(had)H BSM Tag1	11.8	20%	1.67	0.24

H $\rightarrow\gamma\gamma$ AC : VH lep. + MET

Table 8: Definition of the V(lep)H categories based on the values of the discriminants $\mathcal{D}_{\text{STXS}}$ and \mathcal{D}_{BSM} .

Analysis categories	$\mathcal{D}_{\text{STXS}}$ range	\mathcal{D}_{BSM} range
Z(lep)H Tag0	$0.229 < \mathcal{D}_{\text{STXS}}^{\text{ZHlep}} < 1.00$	$-0.68 < \mathcal{D}_{\text{BSM}}^{\text{ZHlep}} < 1.00$
Z(lep)H Tag1	$-0.135 < \mathcal{D}_{\text{STXS}}^{\text{ZHlep}} < 0.229$	$-0.16 < \mathcal{D}_{\text{BSM}}^{\text{ZHlep}} < 1.00$
W(lep)H Tag0	$0.385 < \mathcal{D}_{\text{STXS}}^{\text{WHlep}} < 1.00$	$0.79 < \mathcal{D}_{\text{BSM}}^{\text{WHlep}} < 1.00$
W(lep)H Tag1	$0.385 < \mathcal{D}_{\text{STXS}}^{\text{WHlep}} < 1.00$	$-0.68 < \mathcal{D}_{\text{BSM}}^{\text{WHlep}} < 0.79$
W(lep)H Tag2	$0.125 < \mathcal{D}_{\text{STXS}}^{\text{WHlep}} < 0.385$	$0.89 < \mathcal{D}_{\text{BSM}}^{\text{WHlep}} < 1.00$
W(lep)H Tag3	$0.125 < \mathcal{D}_{\text{STXS}}^{\text{WHlep}} < 0.385$	$-0.68 < \mathcal{D}_{\text{BSM}}^{\text{WHlep}} < 0.89$
V(MET)H Tag0	$0.798 < \mathcal{D}_{\text{STXS}}^{\text{VHMET}} < 1.00$	$0.86 < \mathcal{D}_{\text{BSM}}^{\text{VHMET}} < 1.00$
V(MET)H Tag1	$0.798 < \mathcal{D}_{\text{STXS}}^{\text{VHMET}} < 1.00$	$-1.00 < \mathcal{D}_{\text{BSM}}^{\text{VHMET}} < 0.86$
V(MET)H Tag2	$0.619 < \mathcal{D}_{\text{STXS}}^{\text{VHMET}} < 0.798$	$0.92 < \mathcal{D}_{\text{BSM}}^{\text{VHMET}} < 1.00$
V(MET)H Tag3	$0.619 < \mathcal{D}_{\text{STXS}}^{\text{VHMET}} < 0.798$	$-1.00 < \mathcal{D}_{\text{BSM}}^{\text{VHMET}} < 0.92$

Table 9: The expected number of signal events in the case of SM H with $m_H = 125 \text{ GeV}$ in analysis categories targeting VH associated production in which the vector boson decays leptonically, shown for an integrated luminosity of 138 fb^{-1} . The fraction of the total number of events arising from the VH production mode in each analysis category is provided. Entries with values less than 0.1% are not shown. The σ_{eff} , defined as the smallest interval containing 68.3% of the $m_{\gamma\gamma}$ distribution, is listed for each analysis category. The final column shows the expected ratio of signal to signal-plus-background, $S/(S+B)$, where S and B are the numbers of expected signal and background events in a $\pm 1\sigma_{\text{eff}}$ window centered on m_H .

Analysis categories	H(125) expected signal			
	yield	VH	σ_{eff} (GeV)	S/(S+B)
Z(lep)H Tag0	1.2	99%	1.91	0.45
Z(lep)H Tag1	0.2	82%	2.15	0.06
W(lep)H Tag0	1.4	93%	1.82	0.60
W(lep)H Tag1	5.8	98%	1.96	0.56
W(lep)H Tag2	0.4	64%	1.83	0.15
W(lep)H Tag3	3.6	87%	1.90	0.18
V(MET)H Tag0	1.1	96%	2.06	0.45
V(MET)H Tag1	2.2	96%	2.06	0.40
V(MET)H Tag2	1.2	45%	1.46	0.31
V(MET)H Tag3	6.7	80%	2.05	0.18

[HIG-24-006](#)

H $\rightarrow\gamma\gamma$ AC : ggH

Table 3: List of discriminants for separating anomalous couplings from the SM contribution in the Hgg analysis. The third column indicates the targeted discrimination for that specific observable. For the D_{0-}^{ggH} discriminant, the “ggH” label indicates that this observable is constructed using matrix elements computed for the ggH production process to differentiate it from the equivalent discriminant for the VBF process (D_{0-}^{VBF}). Discriminants in this table are only used for event categorization.

Production mode	Discriminant	Main goal
ggH	D_{0-}^{ggH}	separate between CP -even, CP -odd and mixed CP scenarios
ggH	D_{CP}^{ggH}	differentiate the interference between CP -even and CP -odd
ggH	$D_{\text{STXS}}^{\text{ggH}}$	separate H signal from non-resonant backgrounds
ggH	$D_{\text{bkg}}^{\text{ggH}+2\text{jets}}$	separate between (SM and CP -odd) ggH + 2 jets signal from resonant and non resonant background
ggH	$D_{\text{BSM}}^{\text{ggH}+2\text{jets}}$	separate between BSM CP -odd ggH + 2 jets signal from SM and resonant and non-resonant background

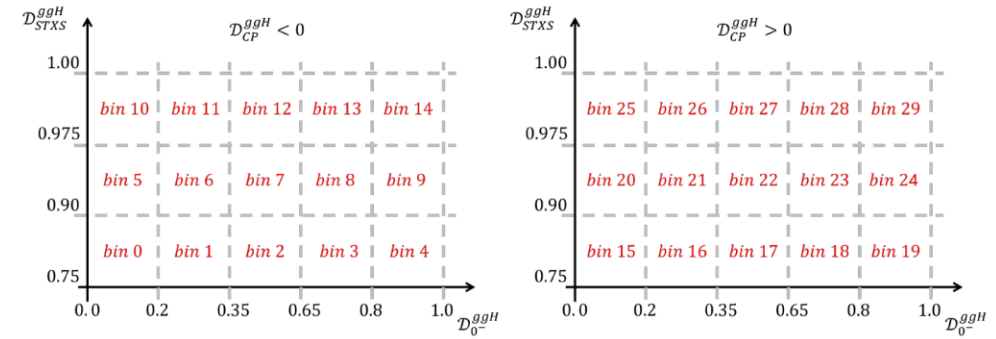
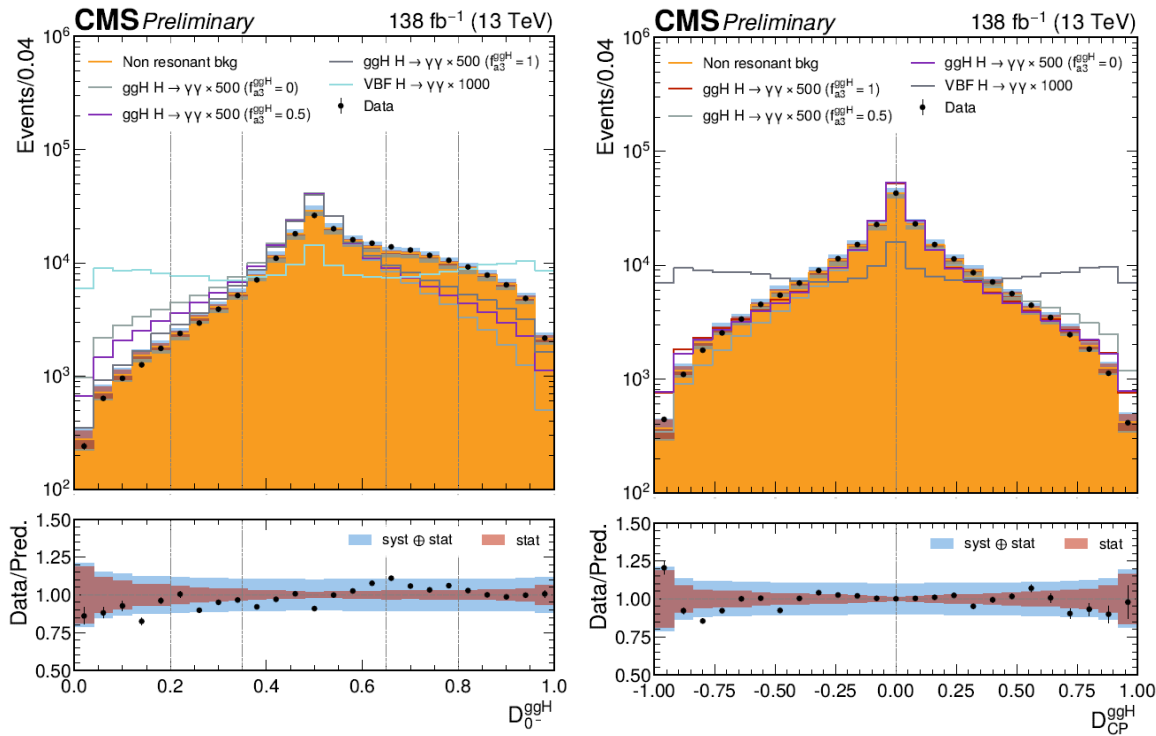


Figure 8: Definition of the Hgg analysis categories defined in bins of D_{0-}^{ggH} and $D_{\text{STXS}}^{\text{ggH}}$ for negative (left) and positive (right) values of D_{CP}^{ggH} .

Table 10: The expected number of signal events in the case of SM H with $m_H = 125\text{ GeV}$ in analysis categories targeting ggH production associated with two jets, shown for an integrated luminosity of 138 fb^{-1} . The fraction of the total number of events arising from the ggH production mode in each analysis category is provided. The σ_{eff} , defined as the smallest interval containing 68.3% of the $m_{\gamma\gamma}$ distribution, is listed for each analysis category. The final column shows the expected ratio of signal to signal-plus-background, $S/(S+B)$, where S and B are the numbers of expected signal and background events in a $\pm 1\sigma_{\text{eff}}$ window centered on m_H .

Analysis categories	H(125) expected signal			
	yield	ggH	σ_{eff} (GeV)	$S/(S+B)$
ggH 0	5.4	39%	2.03	0.07
ggH 1	6.4	62%	2.04	0.04
ggH 2	37.5	81%	2.09	0.04
ggH 3	5.0	75%	2.18	0.04
ggH 4	3.7	66%	2.16	0.07
ggH 5	13.2	34%	1.77	0.17
ggH 6	17.4	60%	1.78	0.09
ggH 7	114.0	77%	1.75	0.08
ggH 8	16.3	70%	1.80	0.09
ggH 9	10.8	60%	1.82	0.16
ggH 10	9.9	29%	1.58	0.37
ggH 11	13.5	59%	1.55	0.27
ggH 12	99.4	72%	1.58	0.26
ggH 13	12.4	63%	1.59	0.28
ggH 14	9.4	46%	1.65	0.39
ggH 15	5.5	37%	2.03	0.07
ggH 16	6.5	61%	2.02	0.04
ggH 17	37.2	80%	2.10	0.03
ggH 18	5.0	74%	2.08	0.04
ggH 19	3.7	64%	2.04	0.07
ggH 20	13.5	36%	1.74	0.18
ggH 21	17.5	60%	1.76	0.09
ggH 22	113.1	77%	1.76	0.08
ggH 23	16.3	70%	1.73	0.09
ggH 24	11.2	59%	1.84	0.15
ggH 25	9.8	29%	1.56	0.38
ggH 26	13.5	58%	1.58	0.26
ggH 27	97.8	73%	1.58	0.25
ggH 28	12.4	63%	1.54	0.28
ggH 29	9.1	46%	1.60	0.40

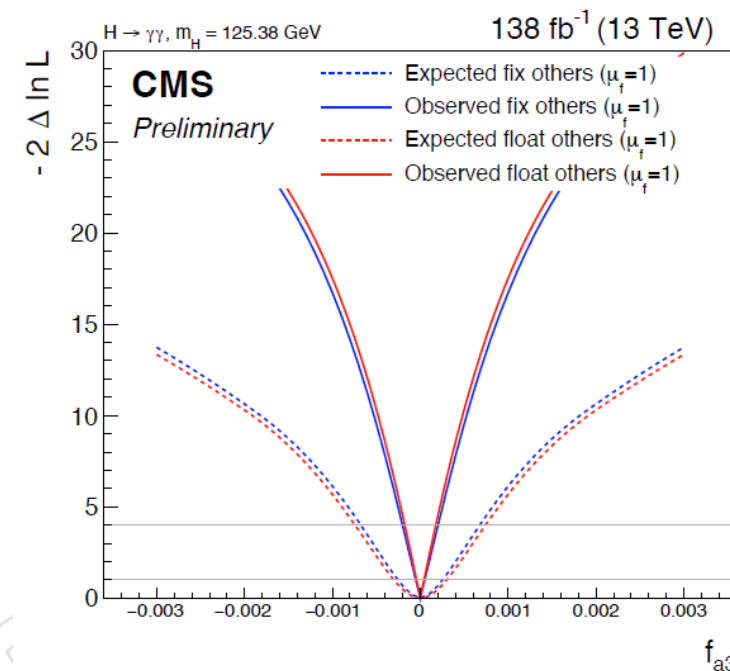
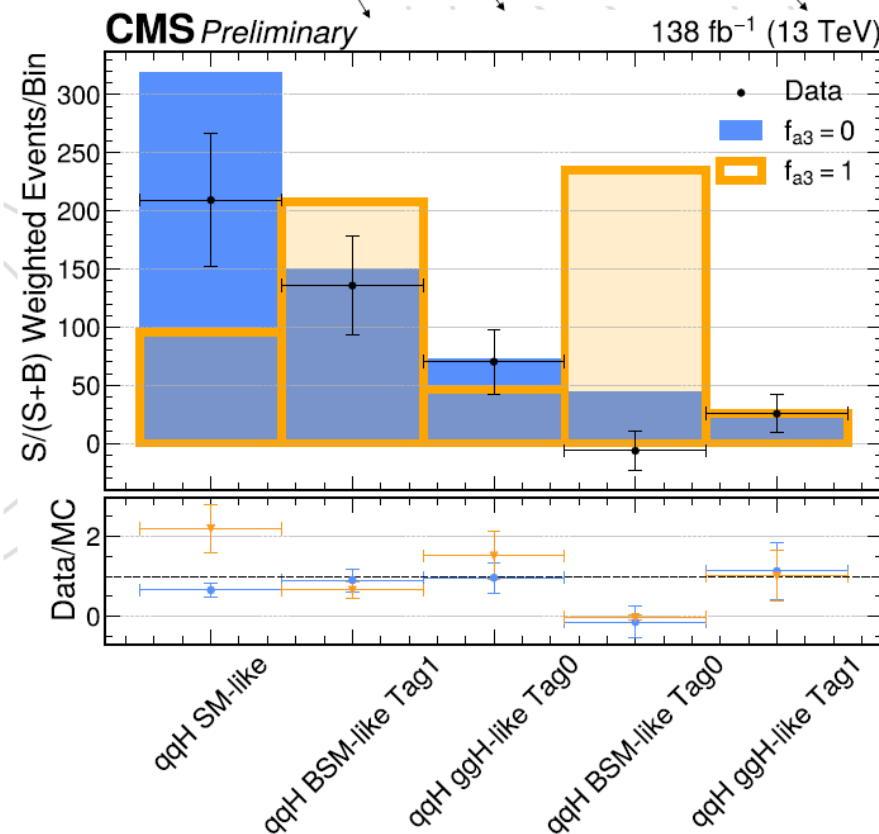
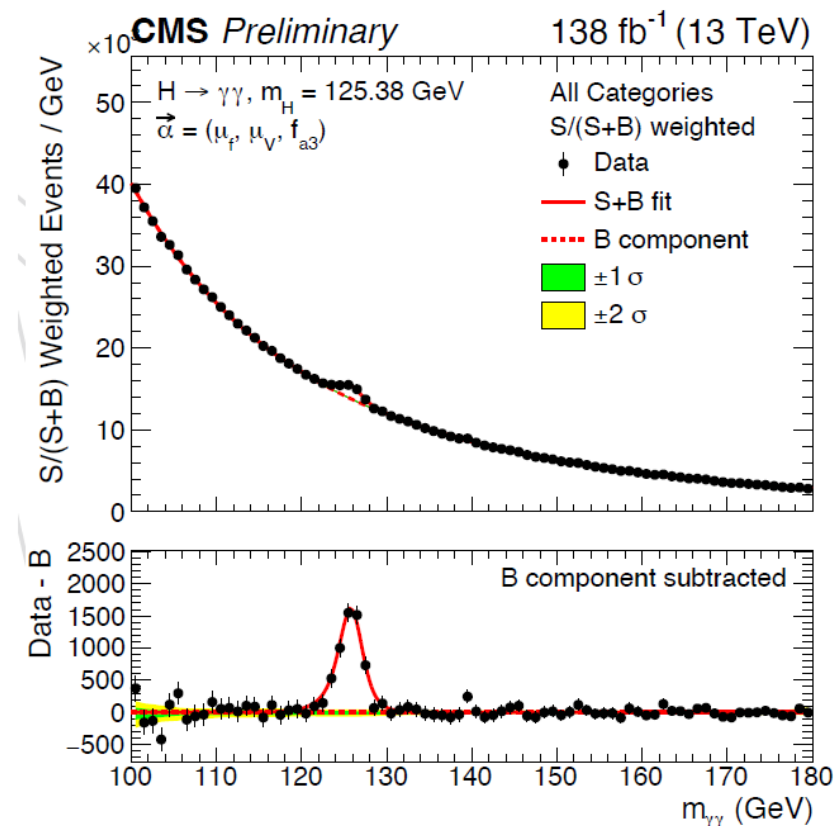


HIG-24-006

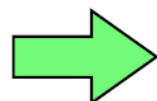
Extraction of Anomalous couplings

f_{ai} -sensitive categories

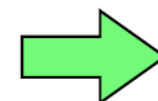
CMS-PAS-HIG-24-006



$m_{\gamma\gamma}$ fit in each category



Bkg-subtracted discriminant^{Bin}

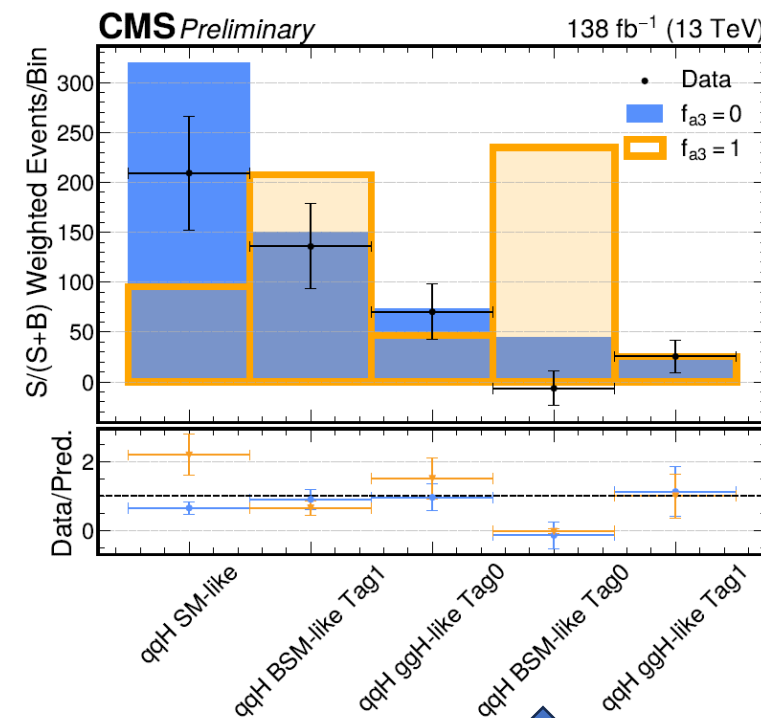
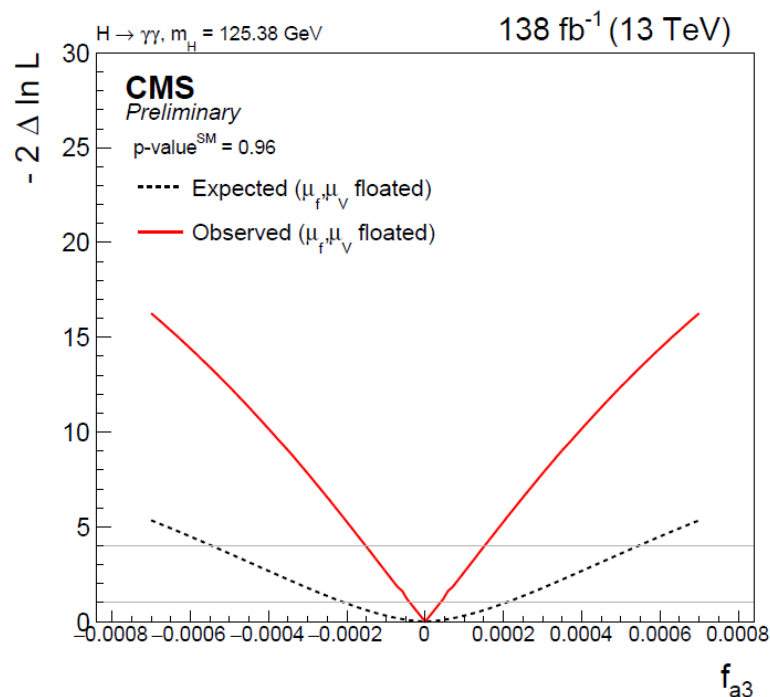


xsec fraction of
anomalous
amplitude²⁸

$H \rightarrow \gamma\gamma$ AC : VBF, VH

The **observed curve** reaches a higher sensitivity than expected

- First, the fitted value of μ_V is **higher than expected ($\mu_V \sim 1.37$)**, mainly due to an *over-fluctuation in the VH channels*, still compatible with the SM expectation
- Second, the categories with the **highest sensitivity to BSM couplings** exhibit an **under-fluctuation** in the observed data



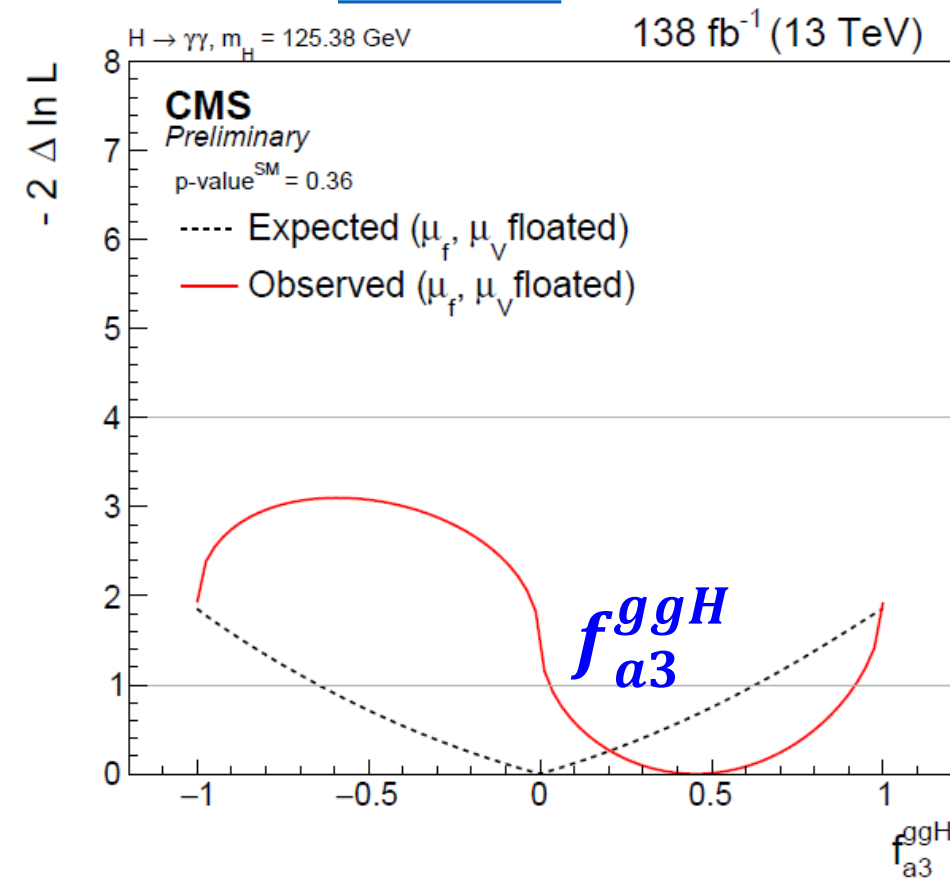
$H \rightarrow \gamma\gamma$ AC : ggH

[HIG-24-006](#)

- The difference in shape between the observed and expected distributions arises from the fact that, by construction, **the value of the negative log-likelihood at $f_{a3}^{ggH} = \pm 1$ is constrained to be the same**

- These points correspond to scenarios where $\mathbf{a_2 = 0}$ and $\mathbf{a_3 = \pm 1}$, in which the BSM contribution is maximal

- The observed data appear to **favour a value around 0.5, rather than 0** as predicted by the SM, which leads to the observed shape



$$f_{a3}^{ggH} = \frac{|a_3^{gg}|^2}{|a_2^{gg}|^2 + |a_3^{gg}|^2} \times \text{sgn} \left(\frac{a_3^{gg}}{a_2^{gg}} \right)$$